Supplementary Information

New Inhibitors for the BPTF Bromodomain Enabled by Structural Biology and Biophysical Assay Development

Peter D. Ycas[1†], Huda Zahid[1†], Alice Chan[2], Noelle M. Olson[1], Jorden A. Johnson[1], Siva K. Talluri[1], Ernst Schonbrunn[2], William C. K. Pomerantz[1*]

Contents

Site Directed Mutagenesis of BPTF plasmid

The His_6-BPTF plasmid was elongated to His_9-BPTF through site-directed mutagenesis. 0.5 µL of 50 nM reverse primers for the pNIC BSA plasmid were combined in a PCR tube with 25 µL of Phusion master mix (DNA polymerase and dNTPS), 0.5 µL of 5 µM forward primer containing the mutation (5'-CAT CAT CAT CAT CAT CAT CAT TCT TCT GGT GTA G- 3'), and 23.5 µL of sterilized H_2O, and 0.5 µL of ~100 ng/ µL template DNA to achieve 20-50 ng of template DNA in the reaction solution.

The PCR tube was then heated to 95° C for 60 s, then cycled from 95° C for 30 s to 60° C for 71 s to 72° C for 90 s 15 times. The tube was then brought to 95° C for 30 s and held at 67° C for 71 s. The tube was then heated to 95° C for 60 s, then cycled from 95° C for 30 s to 67° C for 71 s, to 72° C for 6 min 25 times. The solution was brought to 72° C for 15 min before being cooled and held at 4° C. The resulting DNA was transformed into DH5α cells and grown on agar plates. Colonies were selected and the identity of the mutated plasmid was identified by DNA sequencing.

Example workflow of SPR immobilizations

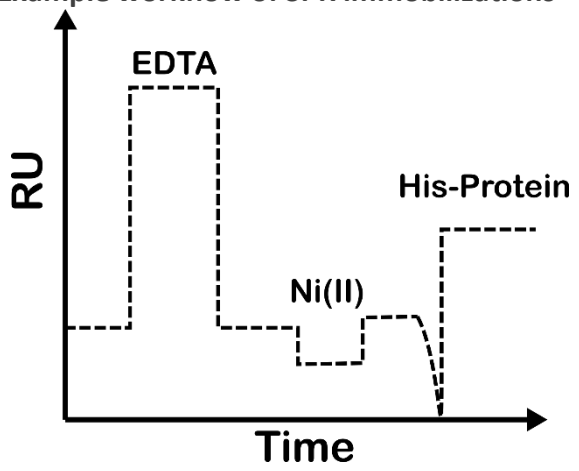

Figure S1: Illustration depicting the theoretical workflow for His_9-protein immobilization. EDTA is passed over to clean the chip surface, Ni (II) is then injected to activate the chip surface, followed by the high affinity His_9-protein which can then be used for protein-ligand analysis.

Comparison of His_6 and His_9 stability on NTA SPR Chip

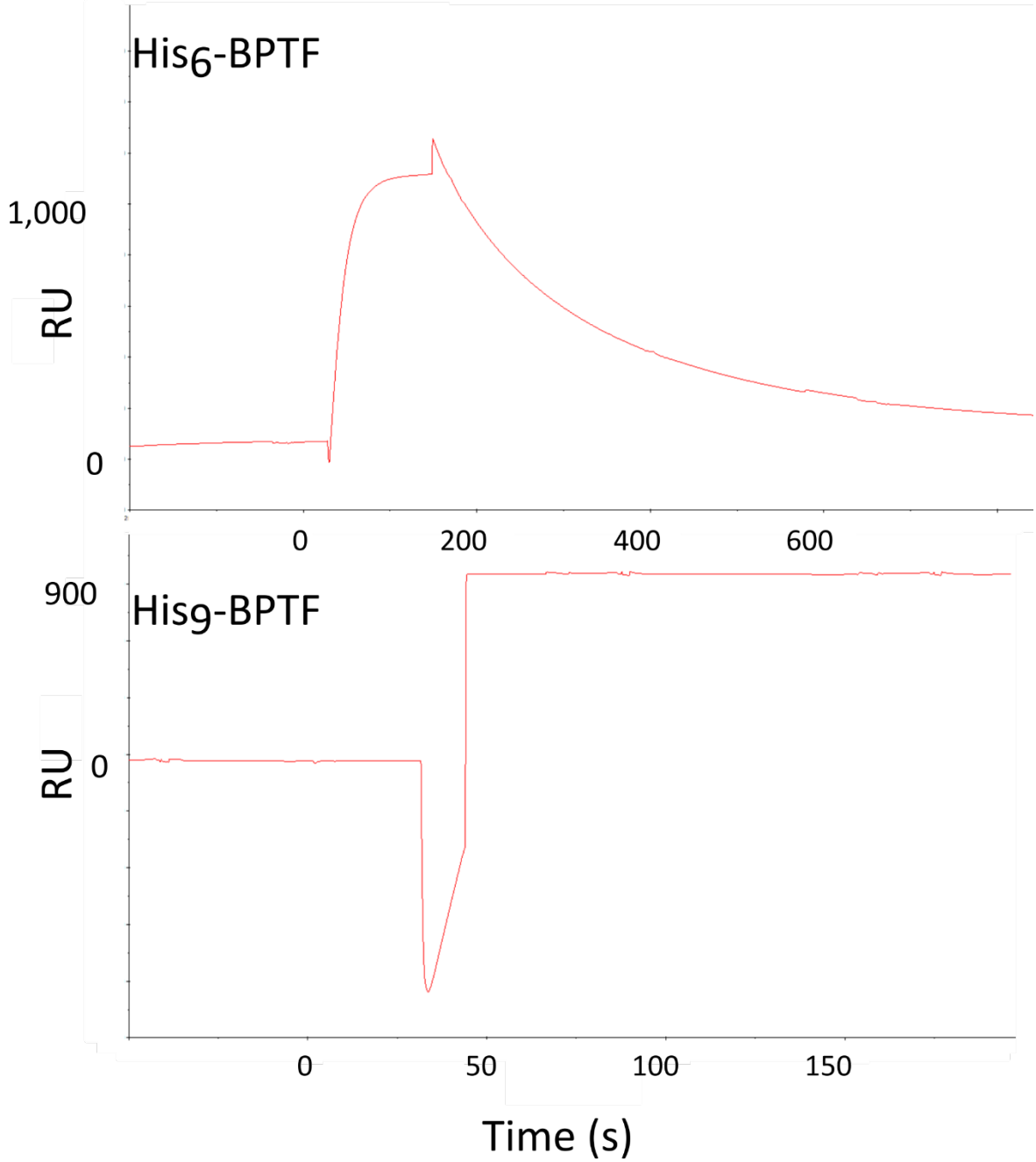

Figure S2: Comparison of the relatively fast dissociation of the His_6-BPTF construct from the SPR chip surface compared to the His_9-BPTF construct. Axes have been normalized to the bulk refractive index of the solution previously passed over the SPR chip surface.

SPR Kinetic Fit of TP-238 (2) binding to His_9-BPTF

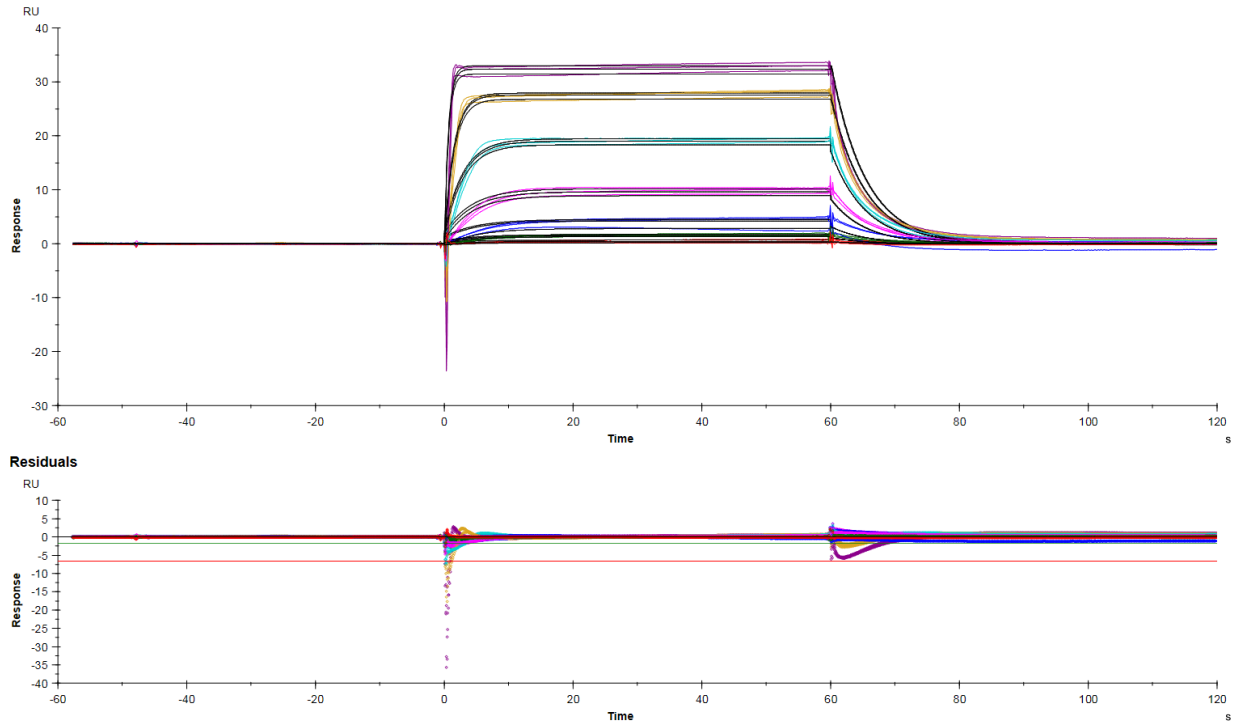

Figure S3: Kinetic fit (top) and residuals comparison (bottom) of (**2**) binding His_9-BPTF. The k_{on} and k_{off} were determined to be $7.17*10^5$ (1/M s) and 0.188 (1/s) respectively, which corresponded to a K_d of $2.62*10^{-7}$ (M).

Effect of DMSO concentration on the SPR assay

Table S1: DMSO concentration effect on bromosporine (**1**) affinity values for unlabeled BPTF and 5FW-BPTF determined by SPR.

DMSO Percentage	Bromosporine Unlabeled BPTF SPR Affinity (µM)	Bromosporine 5FW-BPTF SPR Affinity (µM)
0.5%	7 ± 2	6 ± 2
2%	8 ± 1	13 ± 3

Reproducibility of the SPR assay

Table S2: His_9-BPTF SPR K_d values for repeated experiments. For comparison, values from Tables 1 and 3 are in parentheses

Compound	His_9-BPTF SPR K_d (µM)	His_9-5FW-BPTF SPR K_d (µM)
Bromosporine (1)	13, (9)	17, (19)
GSK4027 (3)	0.8, (1.7)	1.2, (2.3)
(4)	360, (230)	290, (280)

Histone Peptide Synthesis

Peptides were synthesized using standard N-9-Fluorenylmethoxycarbonyl (Fmoc) solid phase synthesis methods on NovaSyn TGR resin (Novabiochem, 0.25 mmol/g) using a Liberty Blue automated microwave synthesizer and *N,N'*-Diisopropylcarbodiimide (DIC) and Oxyma for amino acid activation. All peptides were cleaved from the solid support in a mixture of 95/2.5/2.5 trifluoroacetic acid (TFA)/triisopropylsilane/water for 2-5 hours followed by evaporation of solvent under a nitrogen stream. The crude peptides were precipitated into cold diethyl ether and purified by reverse phase HPLC on a C-18 column using 0.1% TFA water and CH_3CN as solvents (4-24% CH_3CN gradient over 30 minutes). Peptide molecular weight was confirmed using an Ab-Sciex 5800 matrix assisted laser desorption time-of-flight mass spectrometer.

Table S3: Histone peptide sequences and MALDI data.

Peptide	Peptide Sequence	Expected Mass [M/z]	Observed Mass [M+H]
H4 K16ac	H2N-YSGRGKGGKGLGKGGA**K_{ac}**RHRK - C(O)NH_2	2195.26	2196.44
H2AZ.I K4ac,K11ac	H2N-YAGG**K_{ac}**AGKDSG**K_{ac}**AKTKAVSR-C(O)NH2	2062.13	2063.13
H4 K5ac,K8ac,K12ac,K16ac	H2N-YSGRG**Kac**GG**Kac**GLG**Kac**GGA**K_{ac}**RHRK - C(O)NH2	2321.29	2322.42

Peptides HPLC analytical purity traces

Peptide purity was assessed with a Dionex 3000 RP-HPLC system using a Vydac C-18 analytical column and a 0-50% CH_3CN gradient over 50 minutes.

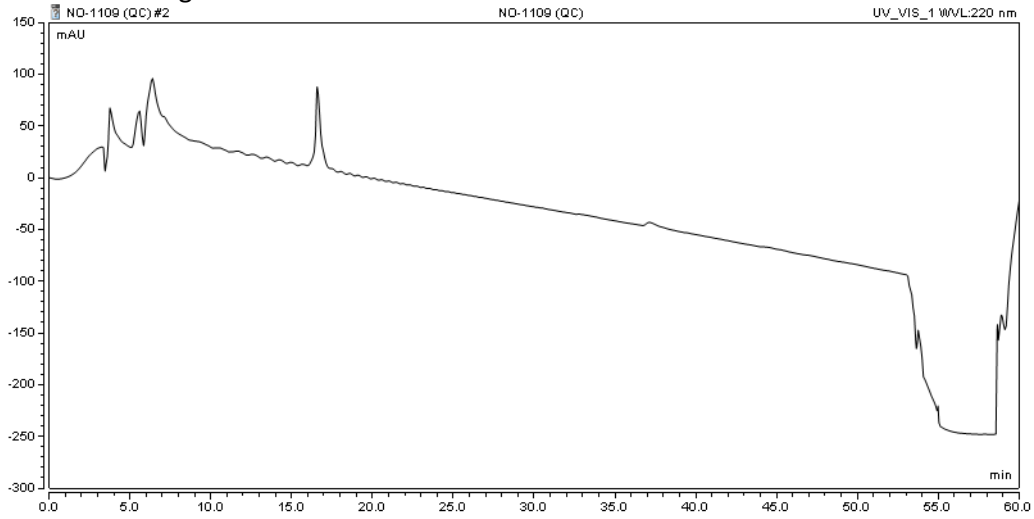

Figure S4: H4 K16ac HPLC trace to assess purity of synthesized peptide.

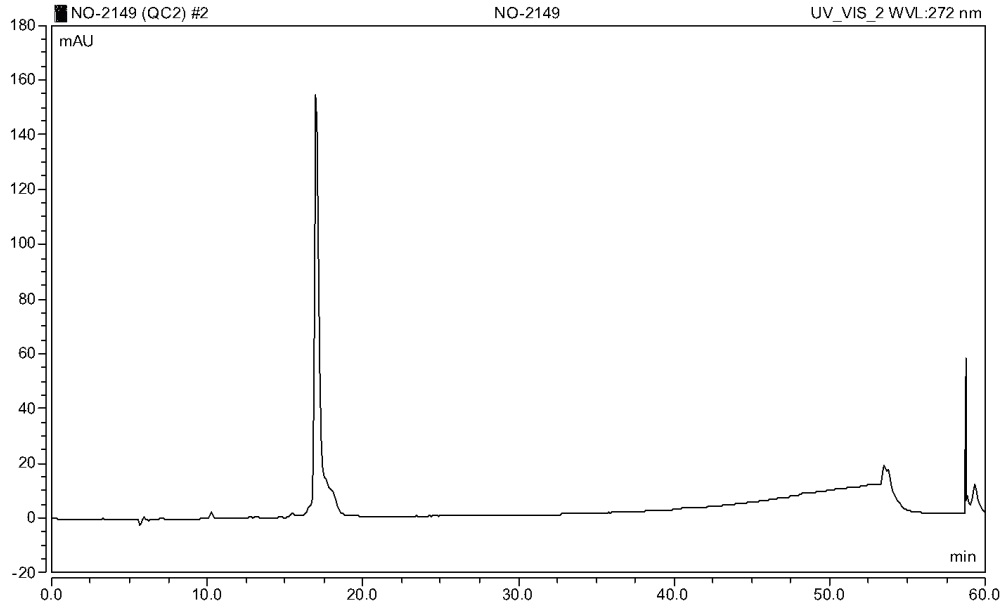

Figure S5: H4 K5ac,K8ac,K12ac,K16ac HPLC trace to assess purity of synthesized peptide.

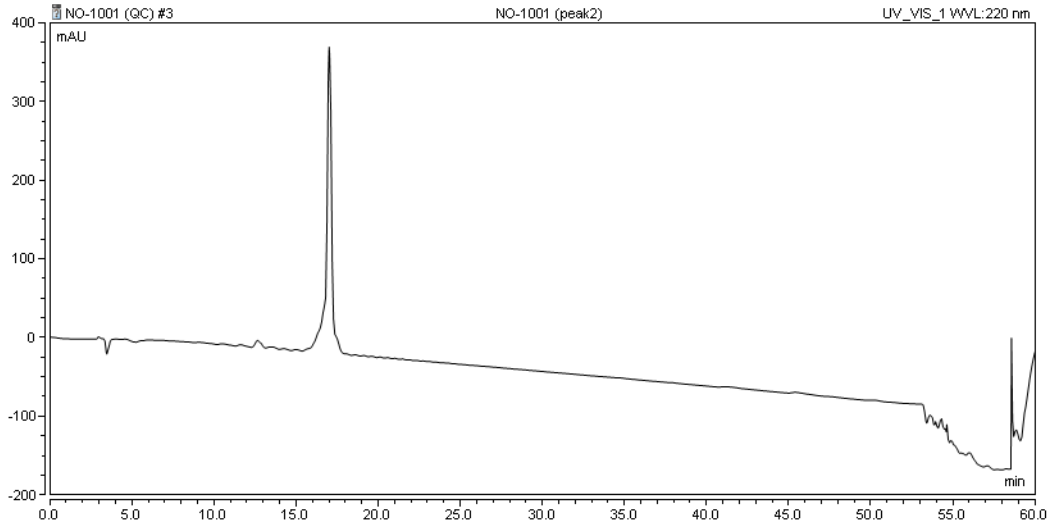

Figure S6: H2AZ.I K4ac,K11ac HPLC trace to assess purity of synthesized peptide.

PrOF NMR titrations of peptides with 5FW-BPTF-

a)

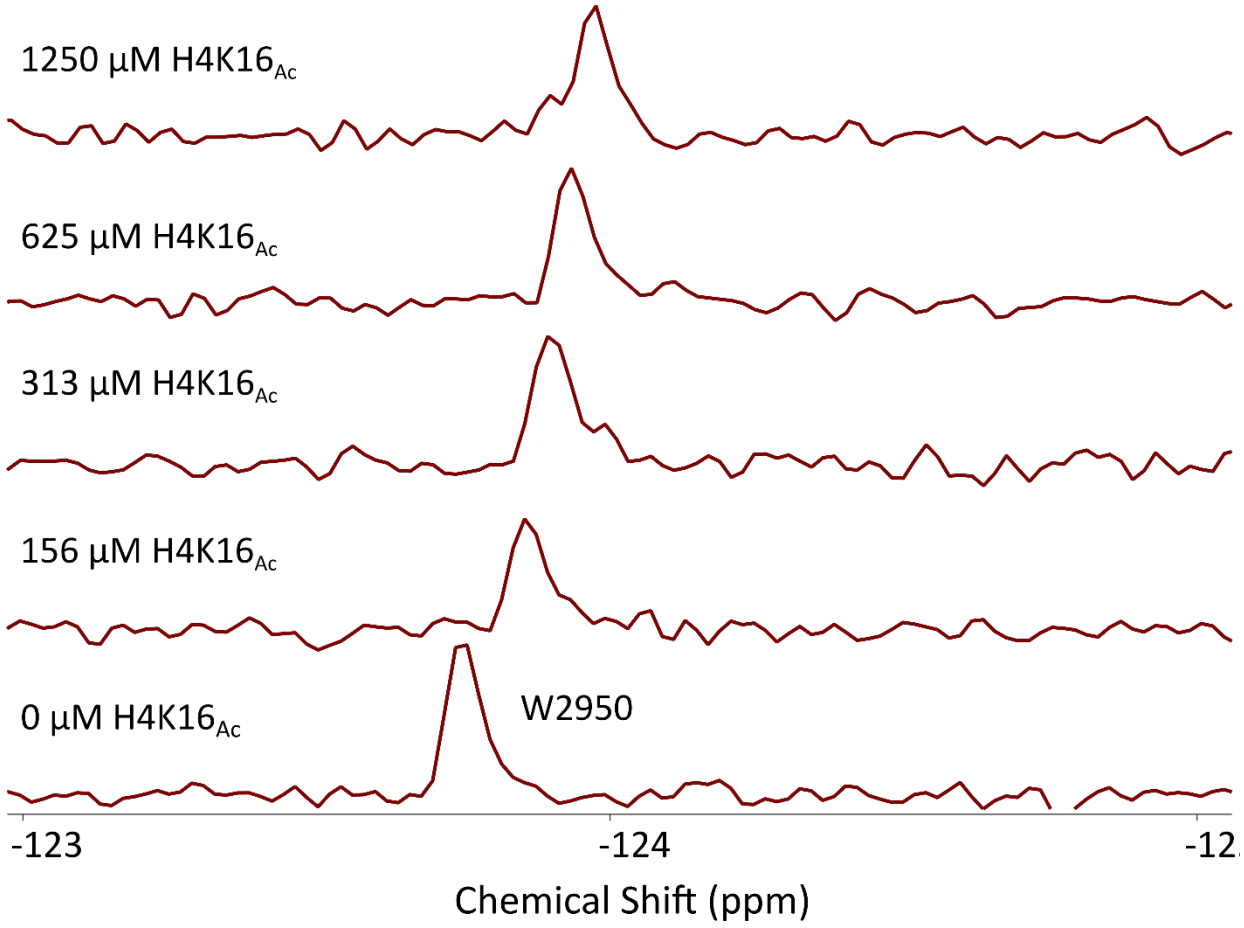

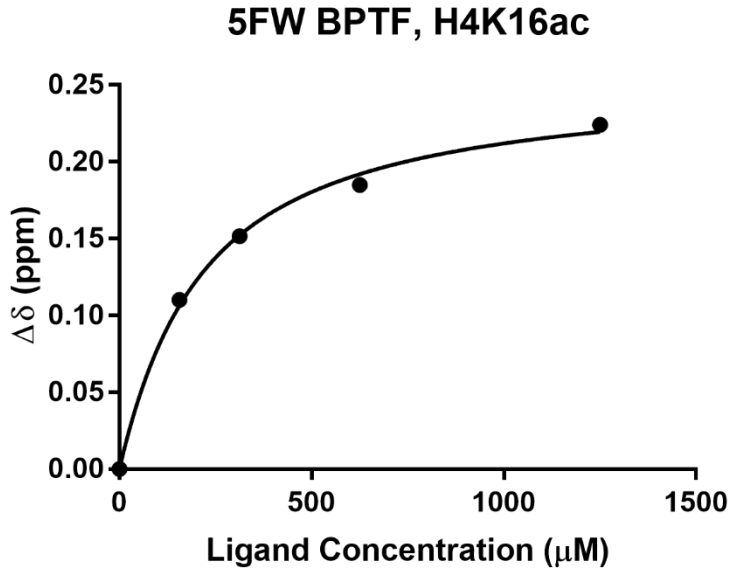

b)

Figure S7: a) PrOF NMR titration of H4 $K16_{Ac}$ with 5FW-BPTF. b) Binding isotherm generated from data displayed in a).

a)

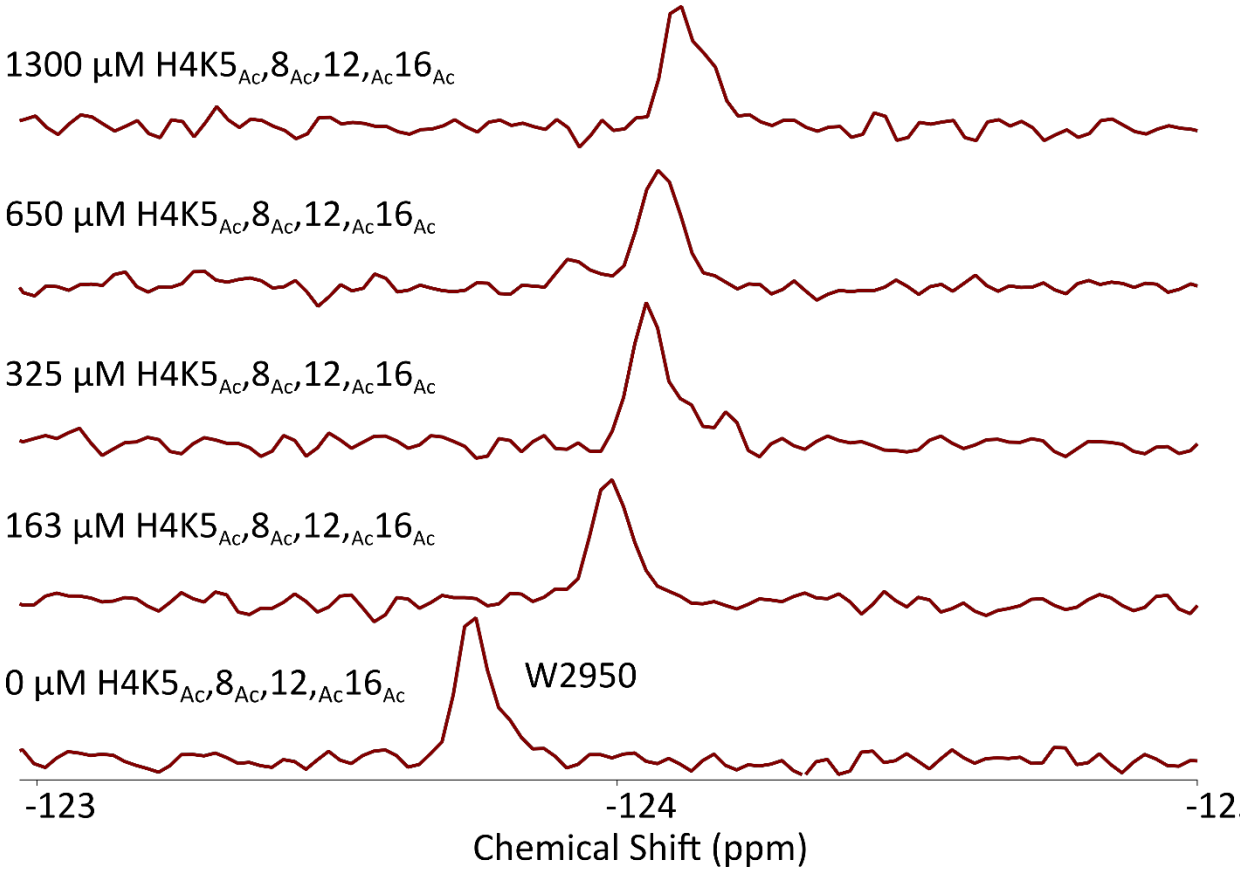

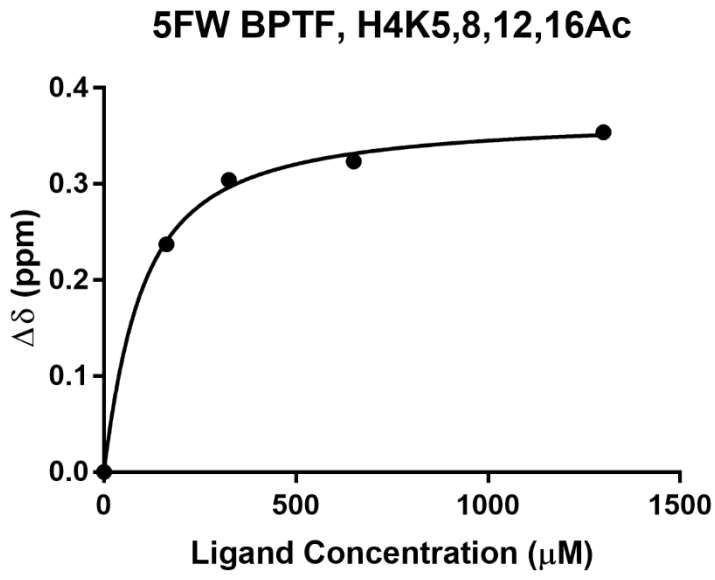

b)

Figure S8: a) PrOF NMR titration of H4 $K5_{Ac},8_{Ac},12_{Ac},16_{Ac}$ with 5FW-BPTF. b) Binding isotherm generated from data displayed in a).

a)

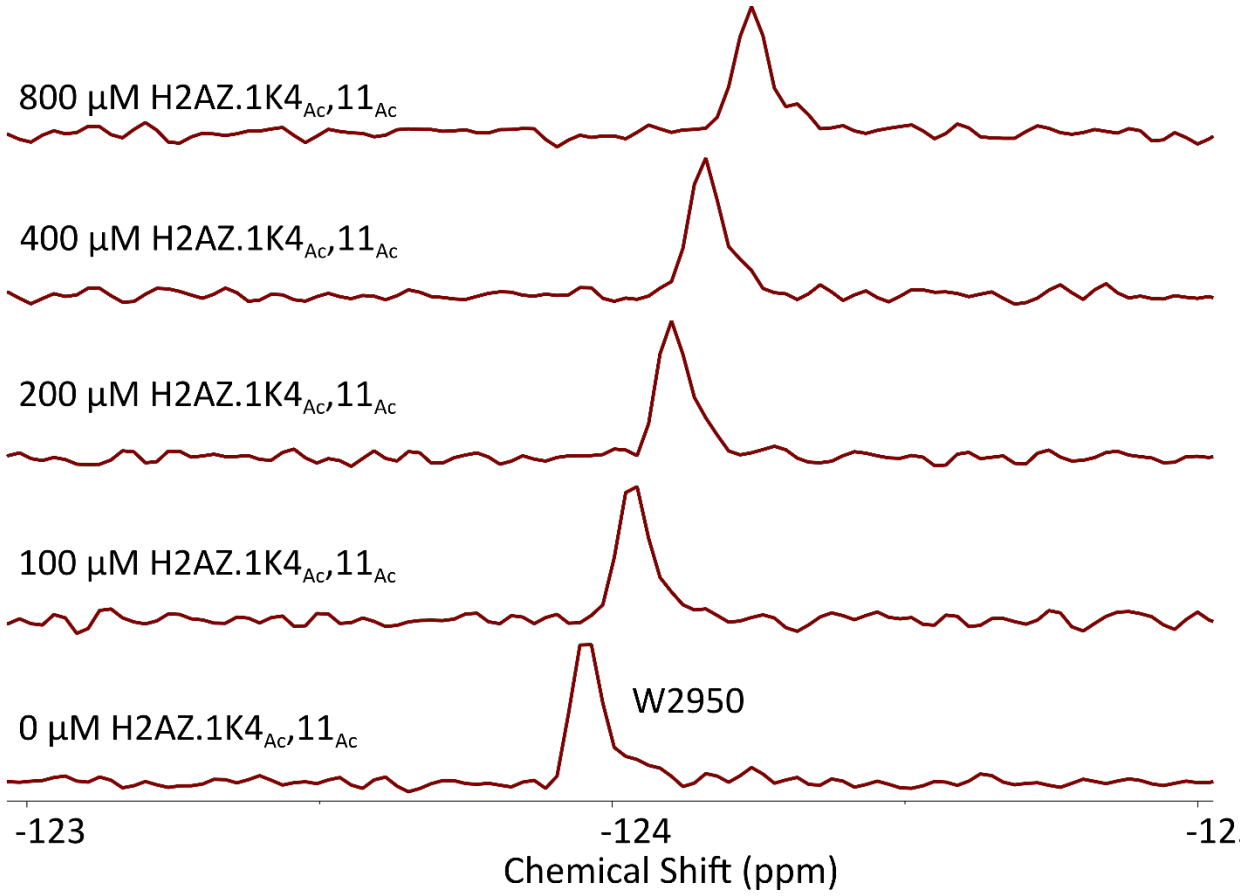

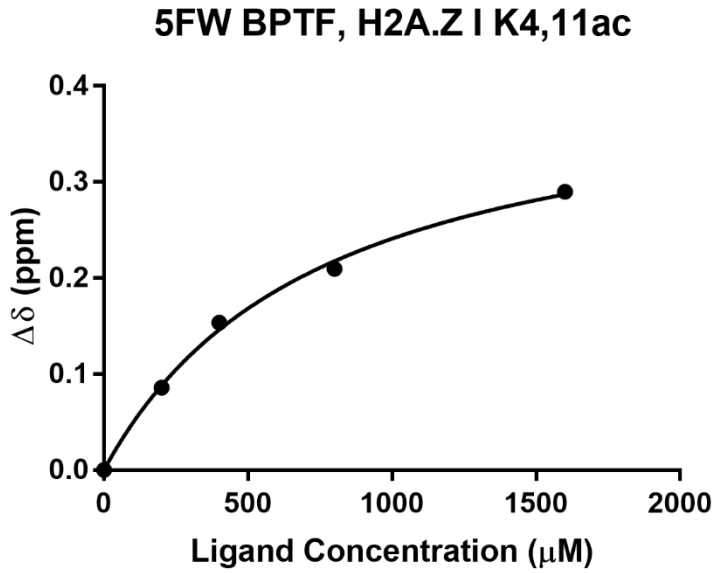

b)

Figure S9: a) PrOF NMR titration of H2AZ.1 K4Ac,11Ac with 5FW-BPTF. b) Binding isotherm generated from data displayed in a).

Small Molecule Synthesis

All commercially available reagents were used without further purification. Flash column chromatography was performed on a Teledyne-Isco Rf-plus CombiFlash instrument with RediSep columns. NMR spectra were collected on a Bruker Avance III AX-400 or a Bruker Avance III HD-500 equipped with a Prodigy TCI cryoprobe or a Bruker Avance III 600 MHz spectrometer. Chemical shifts (δ) were reported in parts per million (ppm) and referenced to residual solvent signals for $CDCl_3$ (^{1}H 7.26 ppm) and DMSO-d_6 (^{1}H 2.50 ppm, ^{13}C 39.5 ppm). Coupling constants (J) are in Hz. Splitting patterns were reported as s (singlet), d (doublet), t (triplet), q (quartet) and m (multiplet). High resolution ESI-MS spectra were recorded on a Waters H-class instrument equipped with a quaternary solvent manager, a Waters sample manager-FTN, a Waters PDA detector and a Waters column manager with an Acquity UPLC protein BEH C18 column (1.7 µm, 2.1 mm x 50 mm). Samples were eluted with a flow rate of 0.3 mL/min. The following gradient was used: A: 0.01% FA in H_2O; B: 0.01% FA in MeCN. 5% B: 0-1 min; 5 to 95% B: 1-7min; 95% B: 7 to 8.5 min. Mass analysis was conducted with a Waters XEVO G2-XS Q-Tof analyzer.

General procedure A for the synthesis of compounds 6-9

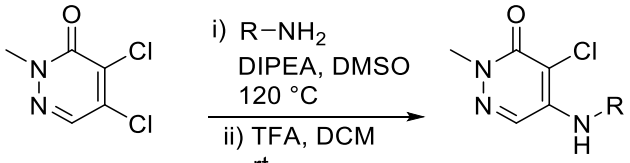

6-9

Step 1: The nucleophilic aromatic substitution procedure was adapted from Humphreys et al.[1] 4,5-dichloro-2-methylpyridazin-3(2H)-one (1.0 eq.) was stirred in DMSO (1 mL) at room temperature, followed by addition of the primary amine (1.2 eq) and *N,N*-Diisopropylethylamine (2.0 eq.). The reaction mixture was heated in a sealed tube at 120 °C for 18 h. Following completion of reaction, the reaction mixture was extracted into ethyl acetate, washed with saturated sodium bicarbonate solution (3×20 mL) and finally with brine (20 mL). The organic layer was dried over magnesium sulfate, filtered, concentrated in vacuo and purified by flash column chromatography (CombiFlash Rf system: 4 g silica, hexanes/ethyl acetate, 0-100% ethyl acetate, 30 minutes). The 4- and 5-positional isomers were obtained, with the 5-positional isomer as the more polar fraction.

Step 2: The product from Step 1 was stirred in DCM (1 mL) at rt, followed by addition of trifluoracetic acid (5.0 eq.) and stirring at rt for 2 h. The DCM was subsequently removed under vacuum and cold diethyl ether was added dropwise to precipitate out the product as a TFA salt. Diethyl ether was removed *in vacuo* to obtain the solid product.

(*R*)-4-chloro-2-methyl-5-((1-methylpiperidin-3-yl)amino)pyridazin-3(2H)-one (6)

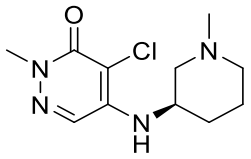

6

Following step 1 of the general procedure A, (4,5-dichloro-2-methylpyridazin-3(2H)-one (100 mg, 0.56 mmol, 1 eq.), (R)-1-methylpiperidin-3-amine (134 mg, 1.12 mmol 2 eq.), *N,N*-Diisopropylethylamine (400 µL, 2.36 mmol, 4.2 eq.), product **6** was obtained as a solid (28 mg, 20% yield) ^{1}H NMR (500 MHz, Chloroform-d) δ 7.54 (s, 1H), 5.23 (s, 1H), 3.75 (s, 3H), 2.62 (s, 2H), 2.51 – 2.36 (m, 4H), 2.29 (s, 3H), 1.84 – 1.66 (m, 2H), 1.65 – 1.49 (m, 1H). ^{13}C NMR (151 MHz, DMSO-d_6) δ 156.7, 143.5, 126.5, 105.1, 59.9, 54.8, 48.1, 45.9, 28.9, 22.2. (solvent obscuring one resonance).

HRMS (ESI-TOF) $[M+H]^+$ m/z calculated for $C_{11}H_{18}ClN_4O^+$ 257.1164, observed 257.1164.

(*S*)-4-chloro-2-methyl-5-(pyrrolidin-3-ylamino)pyridazin-3(2H)-one (7)

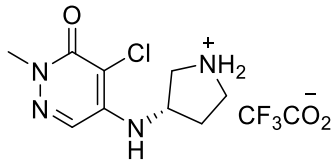

7

Following the general procedure A, (4,5-dichloro-2-methylpyridazin-3(2H)-one (500 mg, 2.79 mmol, 1.0 eq.), tert-butyl (*S*)-3-aminopyrrolidine-1-carboxylate (585 µL, 3.35 mmol, 1.2 eq.), triethylamine (779 µL, 5.59 mmol 2.0 eq.)), product **7** was obtained as a brown solid (310 mg, 49% yield over two steps). ^{1}H NMR (400 MHz, DMSO-d_6) δ 8.93 (s, 2H), 7.92 (s, 1H), 6.55 (d, *J* = 7.7 Hz, 1H), 4.57 – 4.45 (m, 1H), 3.61 (s, 3H), 3.44 (d, *J* = 6.6 Hz, 1H), 3.42 – 3.31 (m, 1H), 3.20 (d, *J* = 24.8 Hz, 2H), 2.33 – 2.18 (m, 1H), 2.04 – 1.90 (m, 1H). ^{13}C NMR (151 MHz, DMSO-d_6) δ 158.7 (q, *J* = 35.1 Hz), 156.9, 143.7, 126.6, 116.1 (q, *J* = 293.3 Hz), 106.1, 51.5, 49.4, 43.9, 30.9.

HRMS (ESI-TOF) $[M+H]^+$ m/z calculated for $C_9H_{14}ClN_4O^+$ 229.0851, observed 229.0854.

(*R*)-4-chloro-2-methyl-5-(pyrrolidin-3-ylamino)pyridazin-3(2H)-one (8)

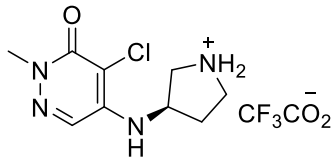

8

Following the general procedure A, (4,5-dichloro-2-methylpyridazin-3(2H)-one (300 mg, 1.68 mmol, 1.0 eq.), tert-butyl (*R*)-3-aminopyrrolidine-1-carboxylate (341 µL, 2.01 mmol, 1.2 eq.), *N,N*-Diisopropylethylamine (584 µL, 3.35 mmol 2.0 eq.)), product **8** was obtained as a white solid (217 mg, 28% yield over two steps). ^{1}H NMR (400 MHz, DMSO-d_6) δ 8.86 (s, 2H), 7.92 (s, 1H), 6.54 (d, *J* = 7.7 Hz, 1H), 4.57 – 4.46 (m, 1H), 3.61 (s, 3H), 3.46 (dd, *J* = 12.2, 6.0 Hz, 1H), 3.36 (q, *J* = 6.0 Hz, 1H), 3.29 – 3.17 (m, 2H), 2.33 – 2.20 (m, 1H), 2.07 – 1.91 (m, 1H). ^{13}C NMR (151 MHz, DMSO-d_6) δ 158.7 (q, *J* = 35.2 Hz), 156.9, 143.7, 126.6, 116.1 (q, *J* = 293.2 Hz), 106.1, 51.5, 49.4, 43.9, 30.9.

HRMS (ESI-TOF) $[M+H]^+$ m/z calculated for $C_9H_{14}ClN_4O^+$ 229.0851, observed 229.0859.

4-chloro-2-methyl-5-(piperidin-1-yl)pyridazin-3(2H)-one (9)

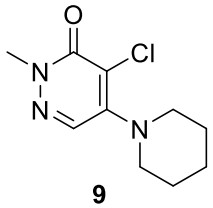

9

Following step 1 of the general procedure A, (4,5-dichloro-2-methylpyridazin-3(2H)-one (100 mg, 0.56 mmol, 1 eq.), piperidine (65 mg, 0.76 mmol, 1.4 eq.), **9** was obtained as a solid (17 mg, 13% yield) ^{1}H NMR (500 MHz, Chloroform-d) δ 7.59 (s, 1H), 3.78 (s, 3H), 3.39 – 3.32 (m, 4H), 1.77 – 1.65 (m, 6H). ^{13}C NMR (151 MHz, DMSO-d_6) δ 157.6, 148.3, 131.4, 114.1, 49.7, 25.6, 23.5. (solvent obscuring one resonance).

HRMS (ESI-TOF) $[M+H]^+$ m/z calculated for $C_{10}H_{15}ClN_3O^+$ 228.0898, observed 228.0903.

cyclopropyl(7-nitro-3,4-dihydroquinolin-1(2H)-yl)methanone (10)

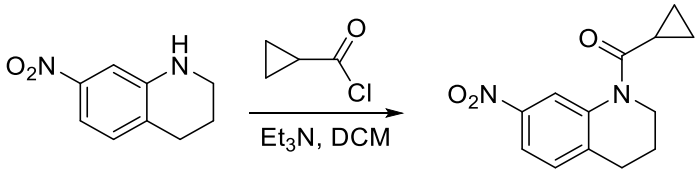

10

7-nitro-1,2,3,4-tetrahydroquinoline (1 g, 5.61 mmol, 1.0 eq.) was dissolved in DCM (7 mL). Triethylamine (3.75 mL, 26.9 mmol, 4.8 eq.) was added and the mixture was cooled to 0 °C. Cyclopropanecarbonyl chloride (1.22 mL, 13.5 mmol, 2.4 eq.) was then added dropwise and the mixture was gradually warmed to room temperature. After stirring at ambient temperature for 16 h, DCM was removed and the crude material was extracted into ethyl acetate. It was washed with brine (3×50 mL) and the organic layer was dried over magnesium sulfate. It was then filtered, concentrated in vacuo and purified by flash column chromatography (CombiFlash Rf system: 12 g silica, hexanes/ethyl acetate, 0-100% ethyl acetate, 20 minutes) to obtain **10** as a yellow solid (1.22 g, 88% yield). ^{1}H NMR (400 MHz, $CDCl_3$) δ 8.38 (d, *J* = 2.4 Hz,

1H), 7.88 (dd, *J* = 8.3, 2.4 Hz, 1H), 7.30 (d, *J* = 8.5 Hz, 1H), 3.86 (d, *J* = 6.5 Hz, 2H), 2.84 (d, *J* = 6.5 Hz, 2H), 2.07 – 1.96 (m, 2H), 1.94 – 1.83 (m, 1H), 1.23 – 1.10 (m, 2H), 0.98 – 0.80 (m, 2H). ^{13}C NMR (151 MHz, DMSO-d_6) δ 172.7, 145.4, 139.3, 139.0, 129.6, 118.7, 118.3, 43.9, 26.9, 22.9, 13.2, 8.5.

HRMS (ESI-TOF) $[M+H]^+$ m/z calculated for C13H15N2O3+ 247.1077, observed 247.1084.

(7-amino-3,4-dihydroquinolin-1(2H)-yl)(cyclopropyl)methanone (4)

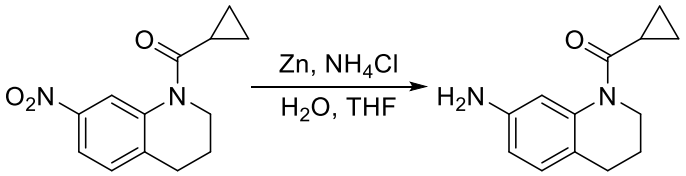

10 **4**

Compound **10** (1 g, 4.06 mmol, 1.0 eq.) was dissolved in 10 mL of THF. Zinc powder (797 mg, 12.1 mmol, 3.0 eq.), ammonium chloride (1.5 g, 28.4 mmol, 7.0 eq.) and 7 mL of distilled water were added. The reaction mixture was heated to reflux for 18 h. Following completion of reaction, zinc was filtered off on celite and the crude material was extracted in ethyl acetate. It was washed with 1 M aqueous sodium hydroxide (3×50 mL) and finally with brine (20 mL). The organic layer was dried over magnesium sulfate, filtered, concentrated in vacuo and purified by flash column chromatography (CombiFlash Rf system: 12 g silica, hexanes/ethyl acetate, 0-100% ethyl acetate, 30 minutes) to afford **4** as a brown solid (506 mg, 58% yield). ^{1}H NMR (400 MHz, CDCl3) δ 6.94 (d, J = 8.1 Hz, 1H), 6.74 (d, J = 2.3 Hz, 1H), 6.47 (dd, J = 8.1, 2.3 Hz, 1H), 3.78 (t, J = 6.6 Hz, 2H), 3.60 (s, 2H), 2.64 (t, J = 6.6 Hz, 2H), 2.05 (tt, J = 8.0, 4.7 Hz, 1H), 1.93 (d, J = 6.7 Hz, 2H), 1.56 (s, 1H), 1.16 – 1.09 (m, 2H), 0.78 (dd, J = 7.9, 3.1 Hz, 2H). ^{13}C NMR (151 MHz, DMSO-d_6) δ 172.0, 146.7, 139.2, 128.7, 119.4, 111.2, 109.9, 42.8, 25.4, 24.0, 13.0, 8.5.

HRMS (ESI-TOF) $[M+H]^+$ m/z calculated for $C_{13}H_{17}N_2O^+$ 217.1335, observed 217.1341.

(7-((2-chloropyrimidin-4-yl)amino)-3,4-dihydroquinolin-1(2H)-yl)(cyclopropyl)methanone (11)

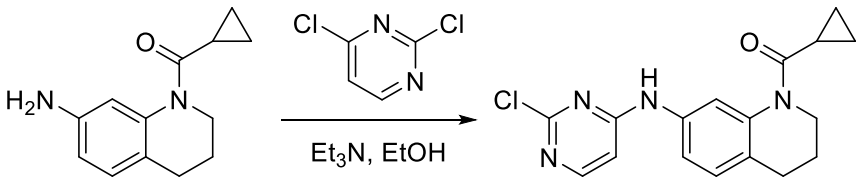

4 **11**

Compound **4** (250 mg, 1.16 mmol, 1.0 eq.) and triethylamine (210 µL, 1.51 mmol, 1.3 eq.) were added to 5 mL of ethanol and the mixture was cooled to 0 °C. 2,4-dichloropyrimidine (190 mg, 1.27 mmol, 1.1 eq.) was then added portion-wise over 5 minutes and the mixture was gradually warmed to room temperature. The reaction mixture was then heated to reflux for 18 h. Following completion of reaction,

ethanol was removed and the crude material was extracted into ethyl acetate. It was washed with saturated sodium bicarbonate solution (3×20 mL) and finally with brine (20 mL). The organic layer was dried over magnesium sulfate, filtered, concentrated in vacuo and purified by flash column chromatography (CombiFlash Rf system: 4 g silica, hexanes/ethyl acetate, 0-100% ethyl acetate, 20 minutes) to afford **11** as a yellow solid (275 mg, 72% yield). ^{1}H NMR (500 MHz, DMSO-d_6) δ 10.00 (s, 1H), 8.20 – 8.01 (m, 1H), 7.79 (s, 1H), 7.20 (s, 2H), 6.73 (d, *J* = 5.9 Hz, 1H), 3.72 (s, 2H), 2.70 (s, 2H), 2.11 (dt, *J* = 8.0, 3.5 Hz, 1H), 1.93 – 1.78 (m, 2H), 0.94 – 0.89 (m, 2H), 0.86 – 0.80 (m, 2H). ^{13}C NMR (126 MHz, DMSO-d_6) δ 172.2, 161.5, 159.4, 157.1, 138.9, 136.2, 128.9, 127.5, 117.0, 116.9, 105.8, 43.0, 25.9, 23.6, 13.1, 8.7. LRMS (ESI-TOF) $[M+Na]^+$ m/z calculated for $C_{17}H_{17}ClN_4NaO^+$ 351.1, observed 351.1.

cyclopropyl(7-((2-(prop-2-yn-1-ylamino)pyrimidin-4-yl)amino)-3,4-dihydroquinolin-1(2H)-yl)methanone (5)

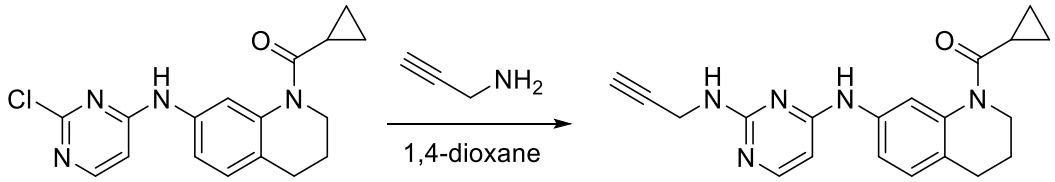

11 **5**

In a sealed reaction vessel, compound **11** (80 mg, 0.243 mmol, 1.0 eq.) was dissolved in 3 mL of 1,4-dioxane. Propargylamine (47 µL, 0.730 mmol, 3.0 eq.) was then added and the reaction mixture was heated at 100 °C for 48 h. The solvent was removed and the crude material was extracted into ethyl acetate. It was washed with saturated sodium bicarbonate solution (2×10 mL) and finally with brine (20 mL). The organic layer was dried over magnesium sulfate, filtered, concentrated in vacuo and purified by flash column chromatography (CombiFlash Rf system: 4 g silica, hexanes/ethyl acetate, 0-100% ethyl acetate, 30 minutes) to afford **5** as a brown oil (24 mg, 28% yield). ^{1}H NMR (500 MHz, DMSO-d_6) δ 9.19 (s, 1H), 7.86 (d, *J* = 5.7 Hz, 1H), 7.73 (s, 1H), 7.58 (s, 1H), 7.10 (d, *J* = 8.3 Hz, 1H), 6.96 (s, 1H), 6.04 (d, *J* = 5.7 Hz, 1H), 4.01 (dd, *J* = 6.1, 2.4 Hz, 2H), 3.71 (t, *J* = 6.5 Hz, 2H), 2.96 (t, *J* = 2.2 Hz, 1H), 2.67 (t, *J* = 6.6 Hz, 2H), 2.08 – 2.00 (m, 1H), 1.85 (q, *J* = 6.5 Hz, 2H), 0.91 (t, *J* = 3.8 Hz, 2H), 0.79 (dq, *J* = 7.4, 3.6 Hz, 2H). ^{13}C NMR (151 MHz, DMSO-d_6) δ 172.2, 161.4, 160.6, 156.1, 138.8, 138.2, 128.4, 125.6, 116.3, 115.6, 82.7, 71.8, 43.0, 30.2, 25.7, 23.8, 13.1, 8.5. (solvent obscuring one resonance).

HRMS (ESI-TOF) $[M+H]^+$ m/z calculated for $C_{20}H_{22}N_5O^+$ 348.1819, observed 348.1820.

^{1}H and ^{13}C NMR spectra of small molecule analogues

4, ^{1}H NMR (400 MHz, $CDCl_3$)

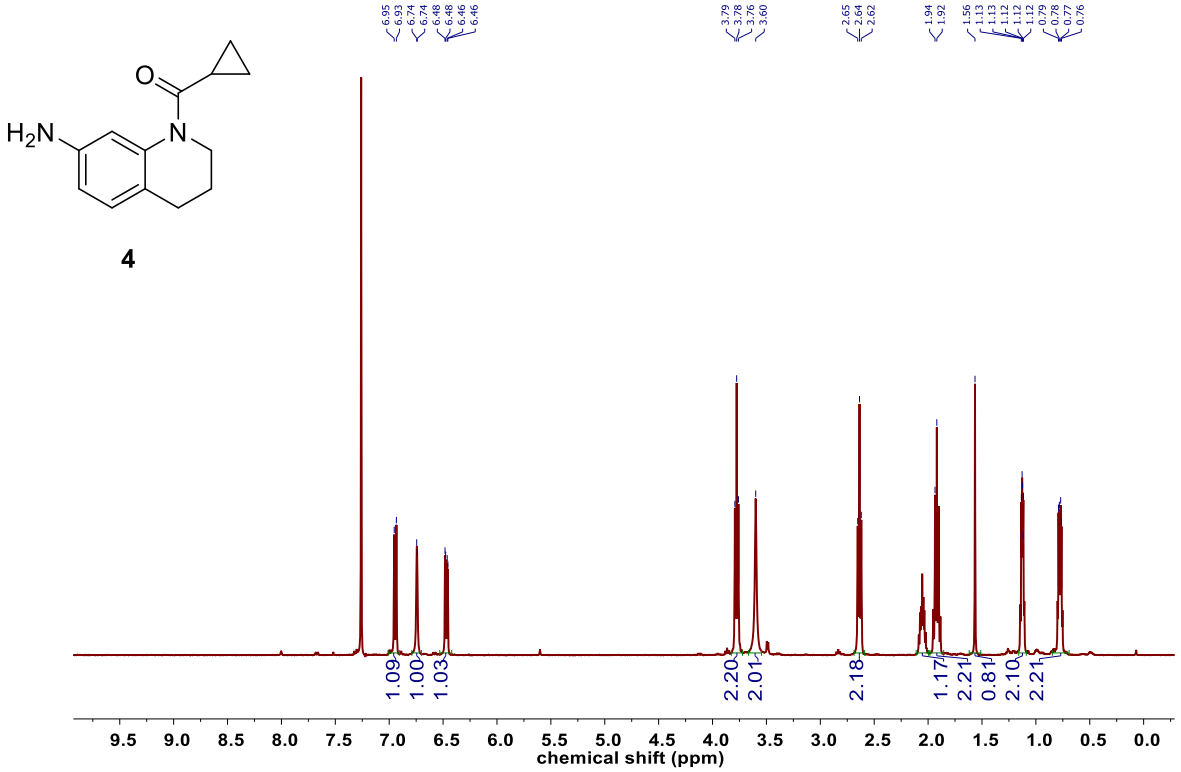

4

4, ^{13}C NMR (151 MHz, DMSO-d_6)

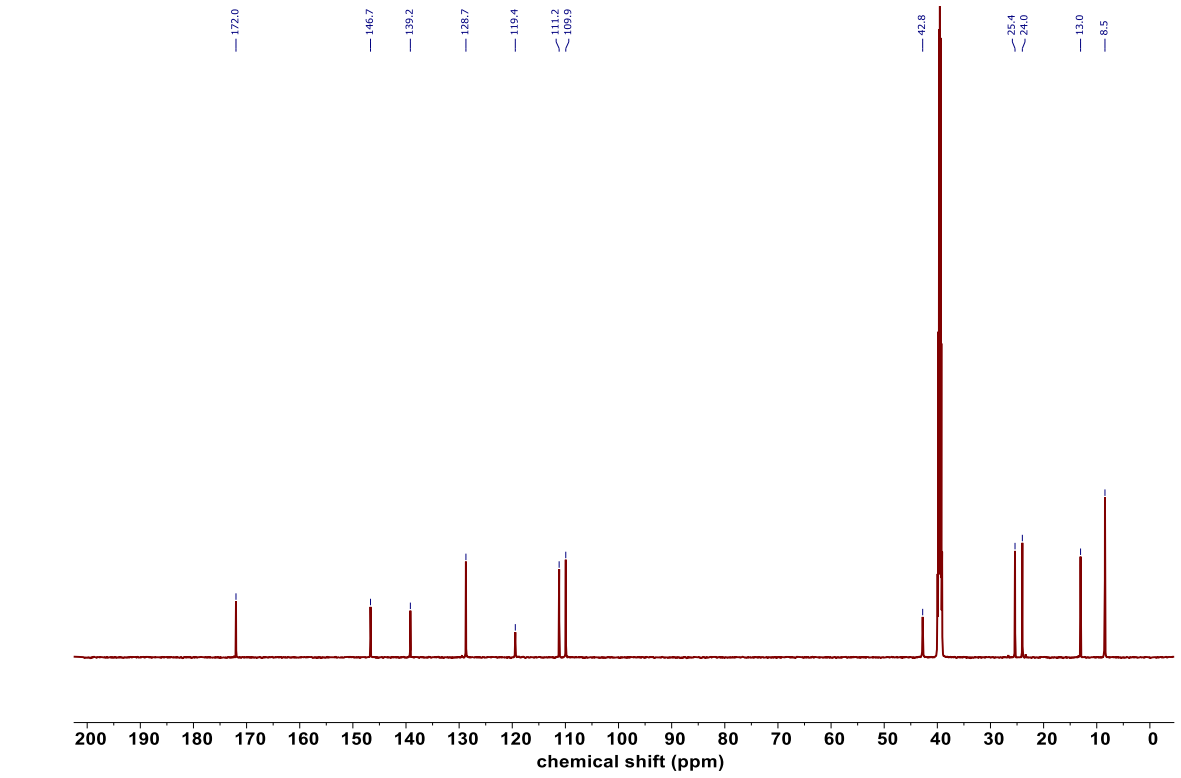

5, ^{1}H NMR (500 MHz, DMSO-d_6)

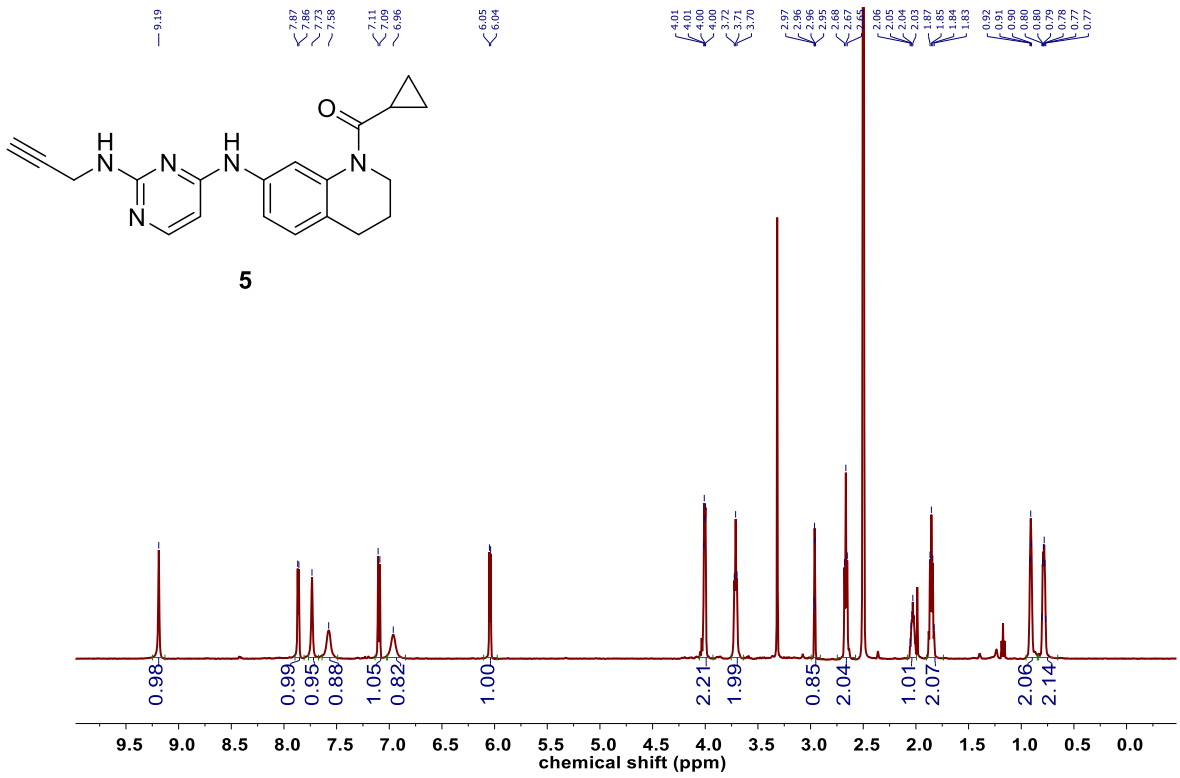

5

5, ^{13}C NMR (151 MHz, DMSO-d_6)

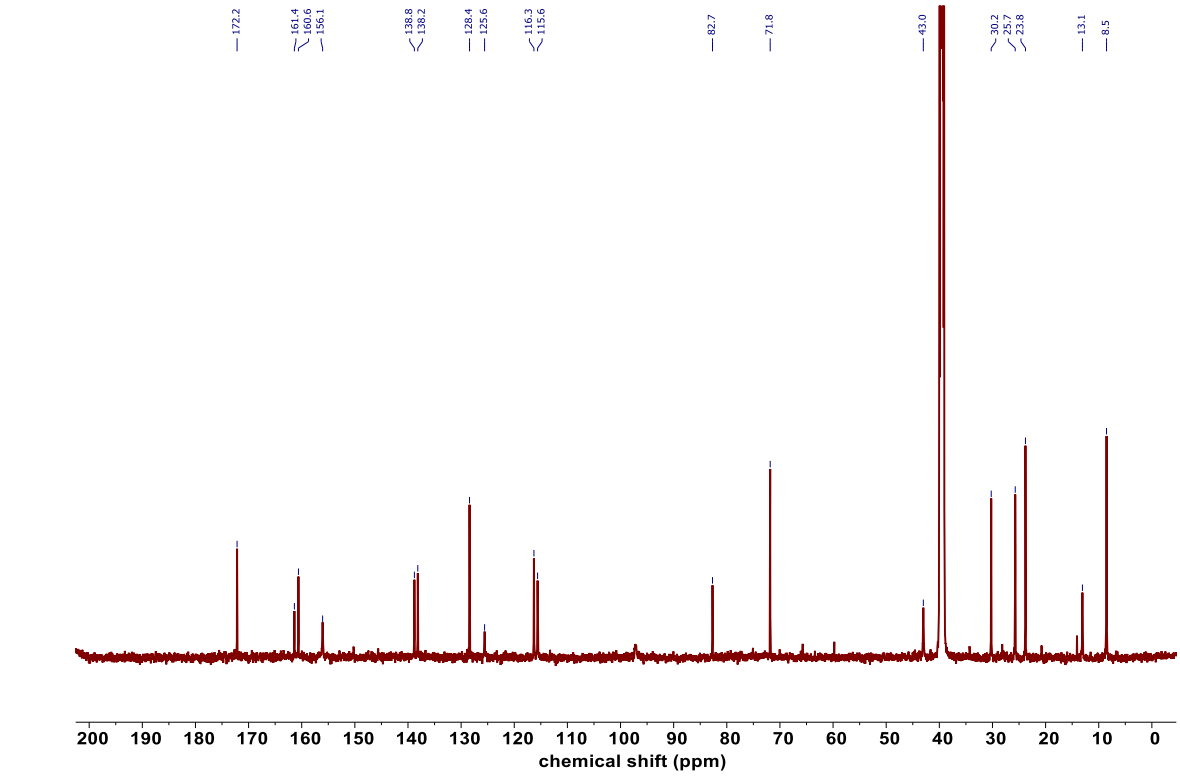

6, ^{1}H NMR (500 MHz, $CDCl_3$)

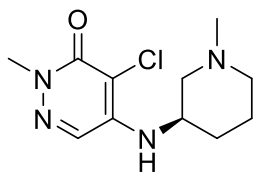

6

6, ^{13}C NMR (151 MHz, DMSO-d_6)

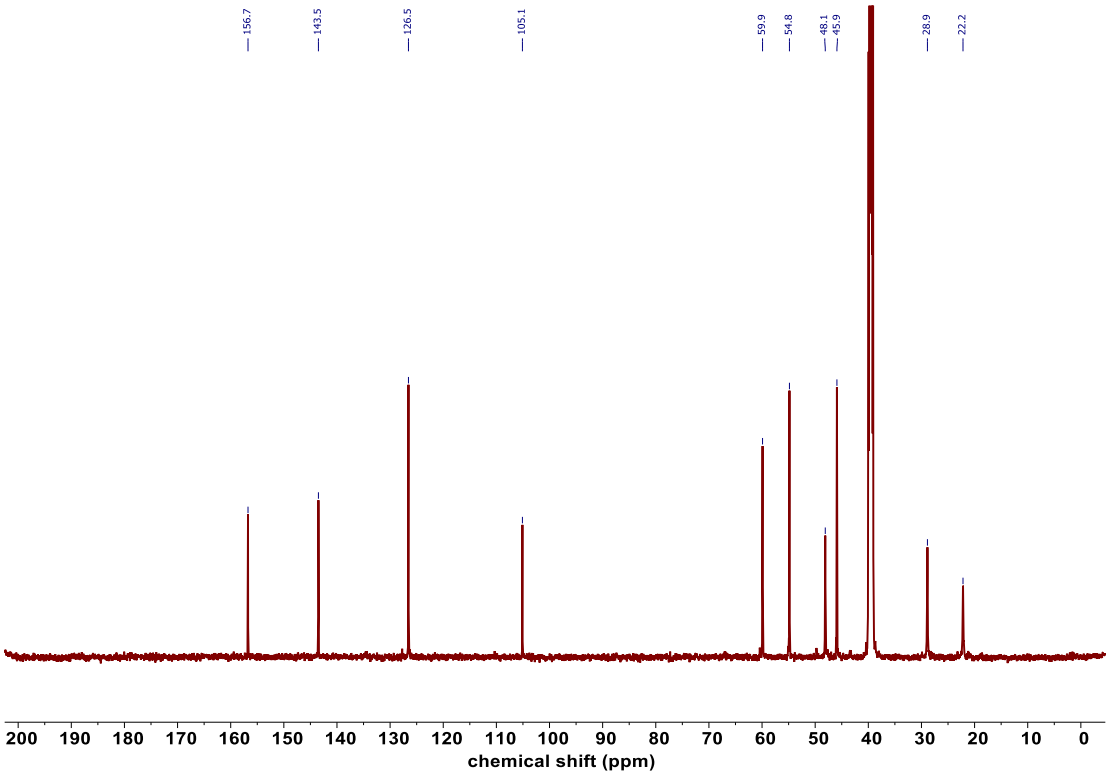

7, ^{1}H NMR (400 MHz, DMSO-d_6)

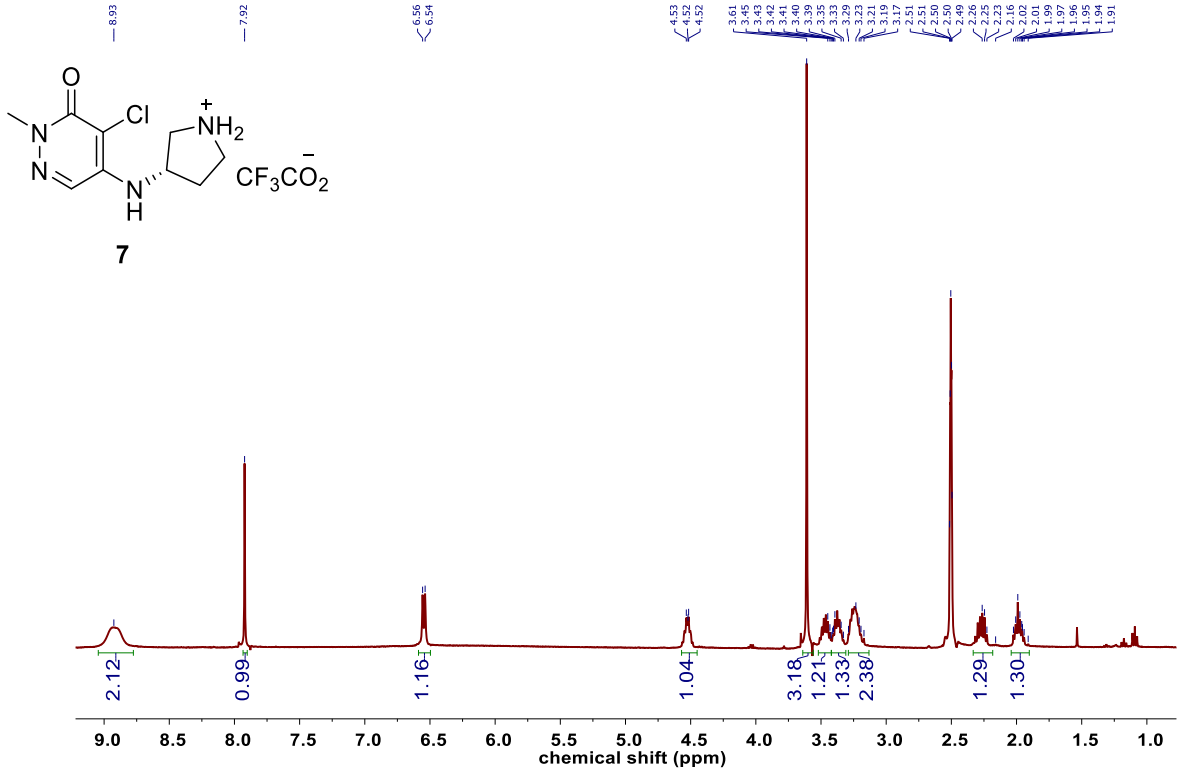

7, ^{13}C NMR (151 MHz, DMSO-d_6)

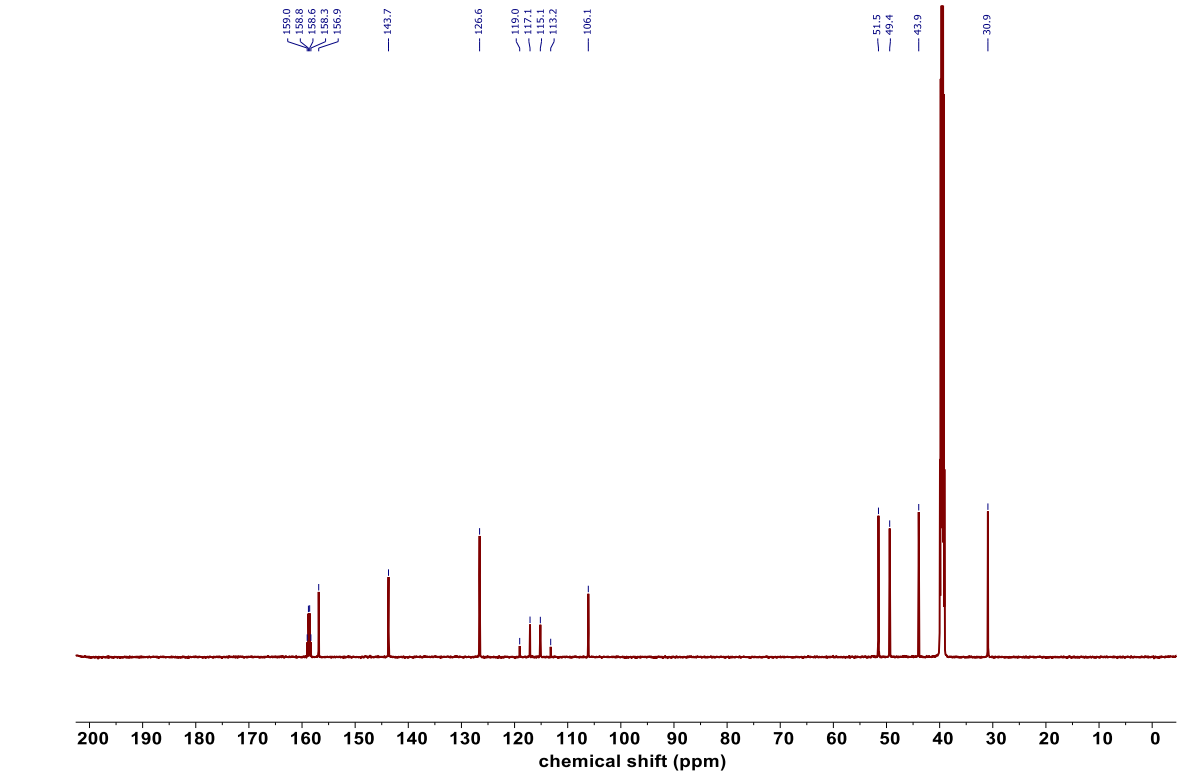

8, ^{1}H NMR (400 MHz, DMSO-d_6)

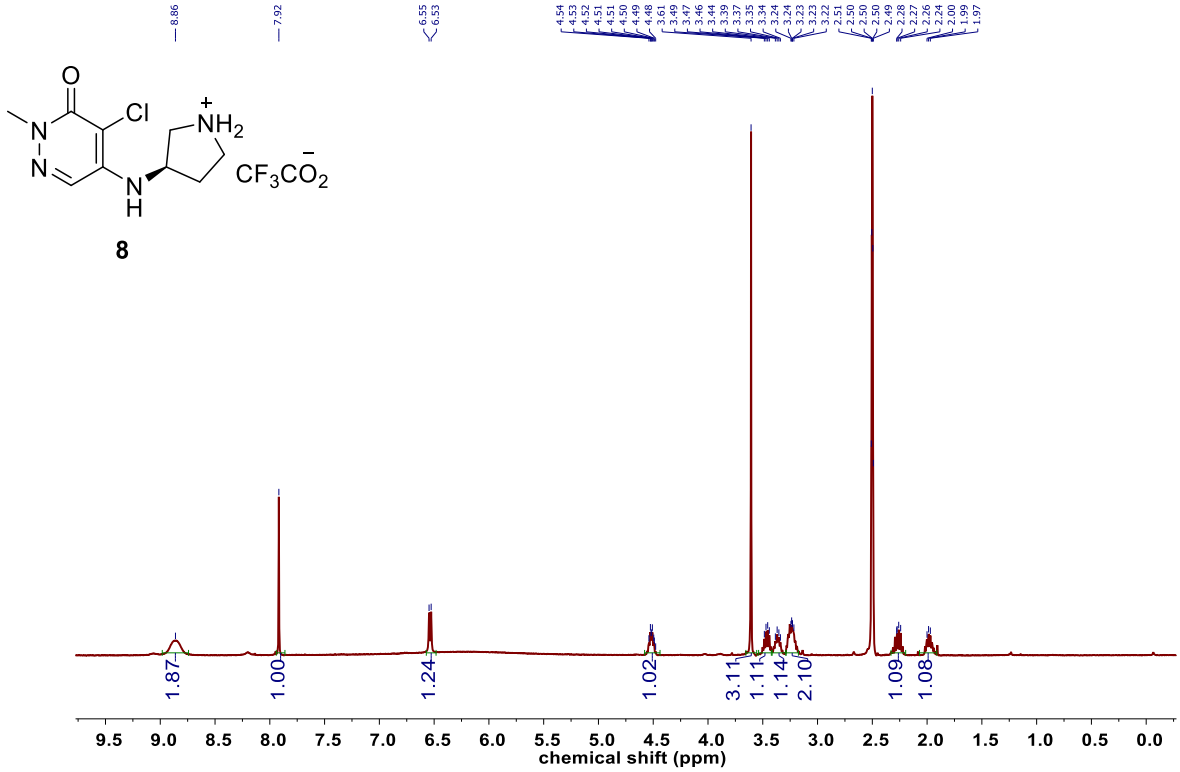

8, ^{13}C NMR (151 MHz, DMSO-d_6)

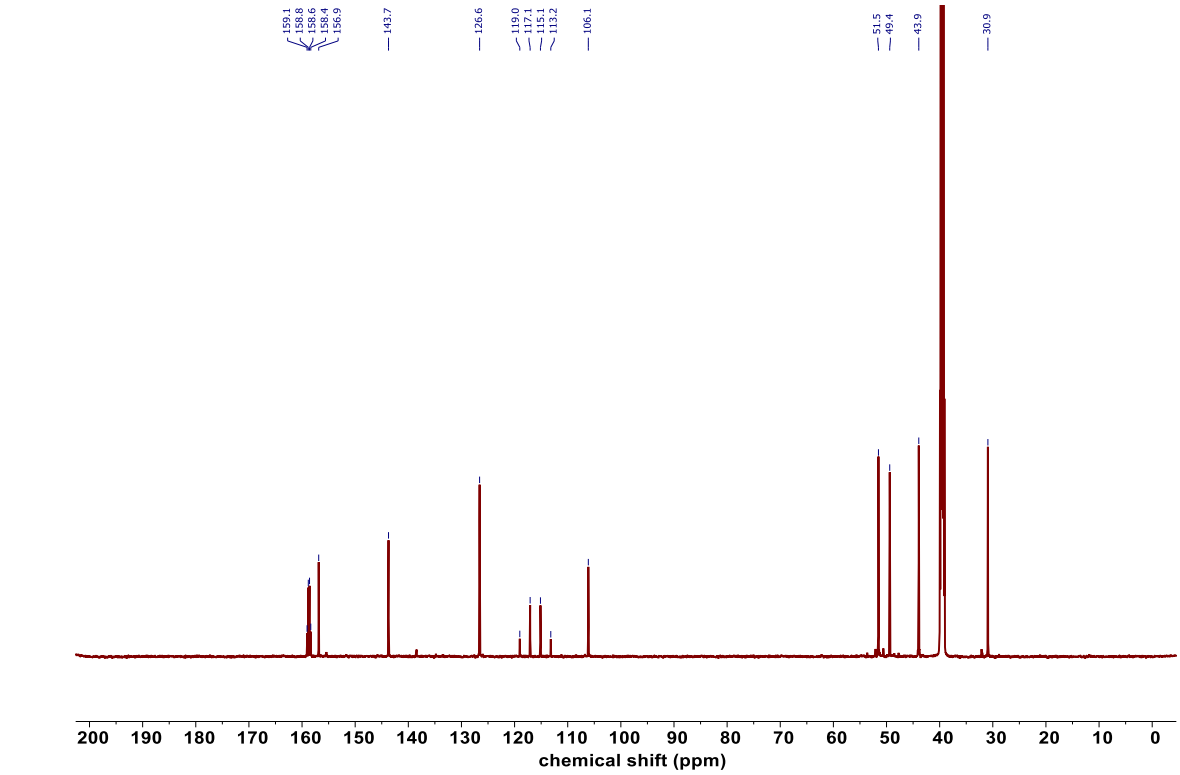

9, ^{1}H NMR (500 MHz, $CDCl_3$)

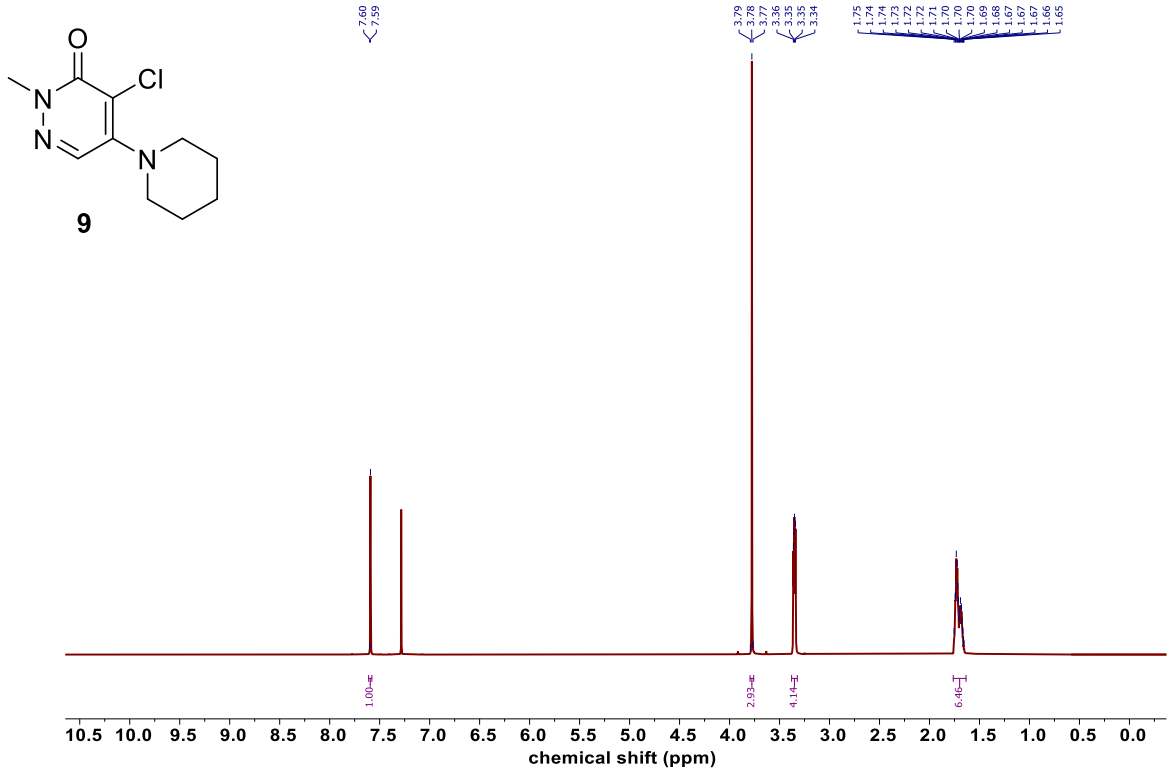

9, ^{13}C NMR (151 MHz, DMSO-d_6)

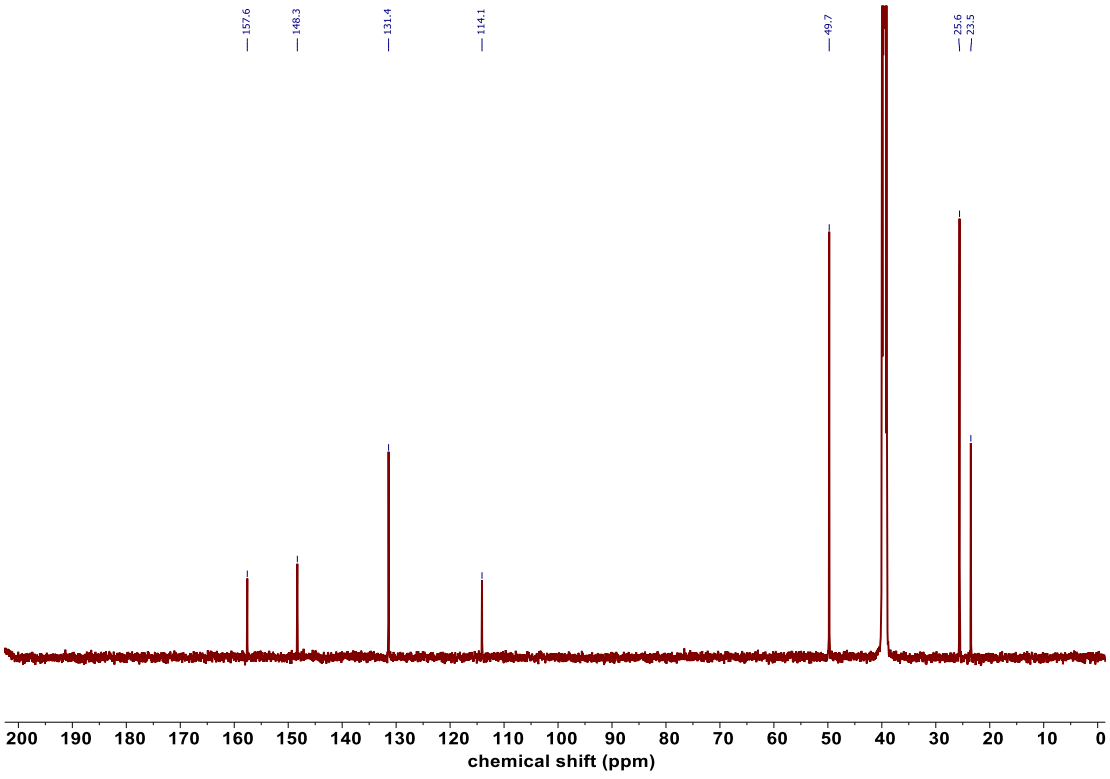

10, ^{1}H NMR (400 MHz, $CDCl_3$)

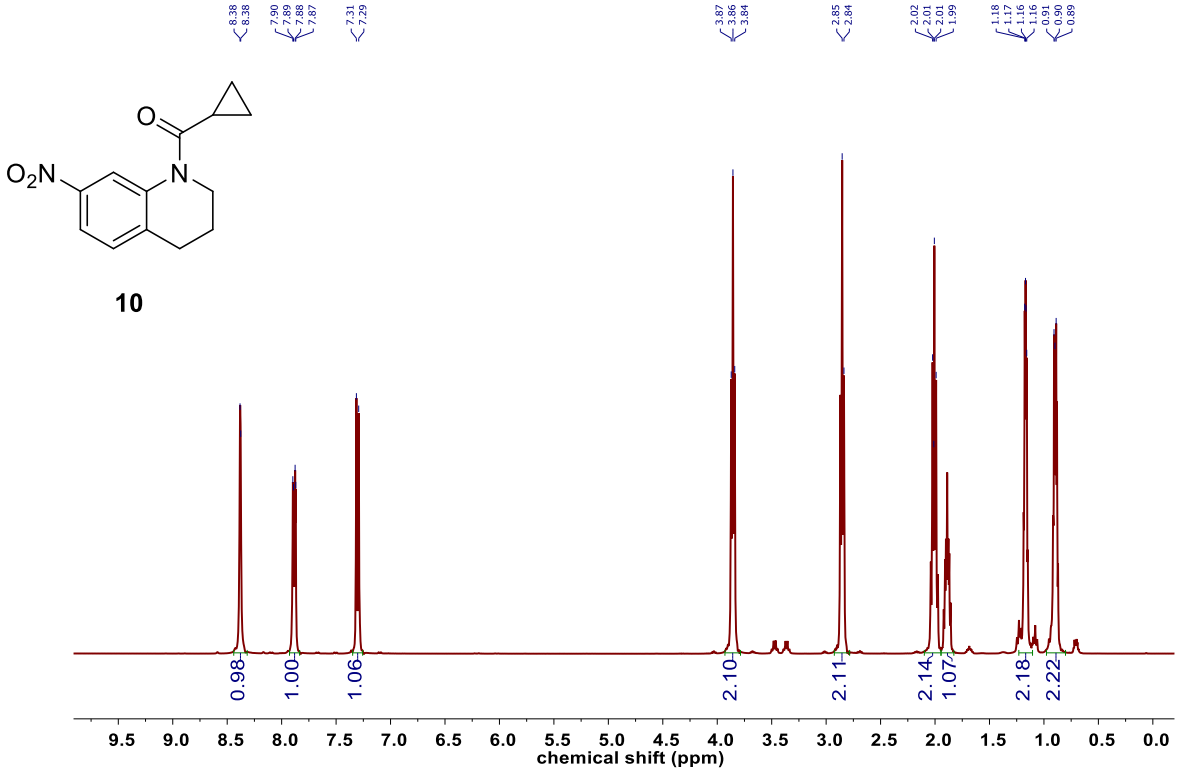

10, ^{13}C NMR (151 MHz, DMSO-d_6)

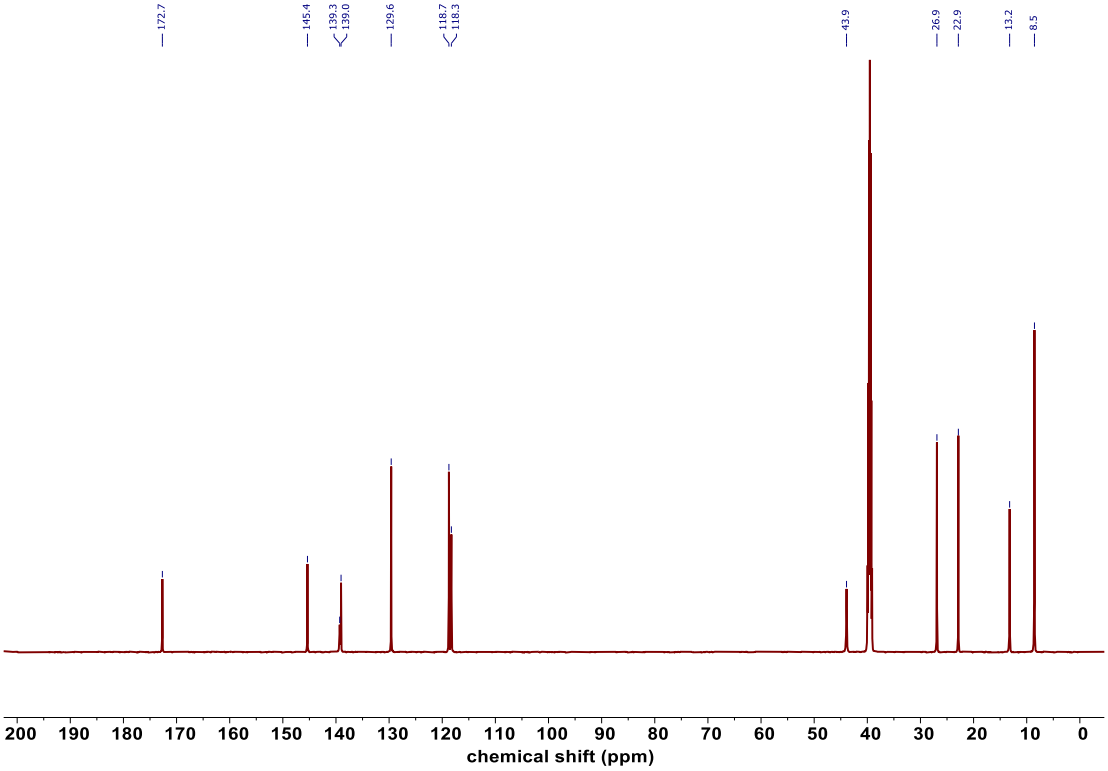

11, ^{1}H NMR (500 MHz, DMSO-d_6)

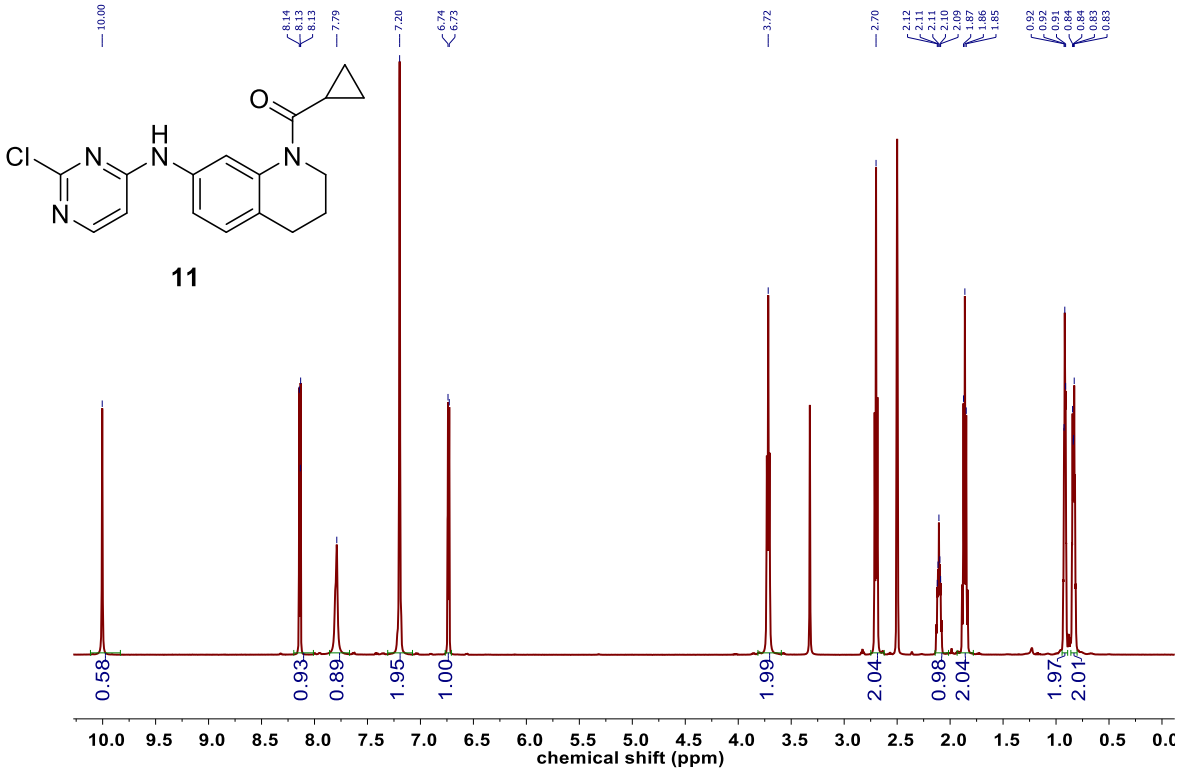

11, ^{13}C NMR (126 MHz, DMSO-d_6)

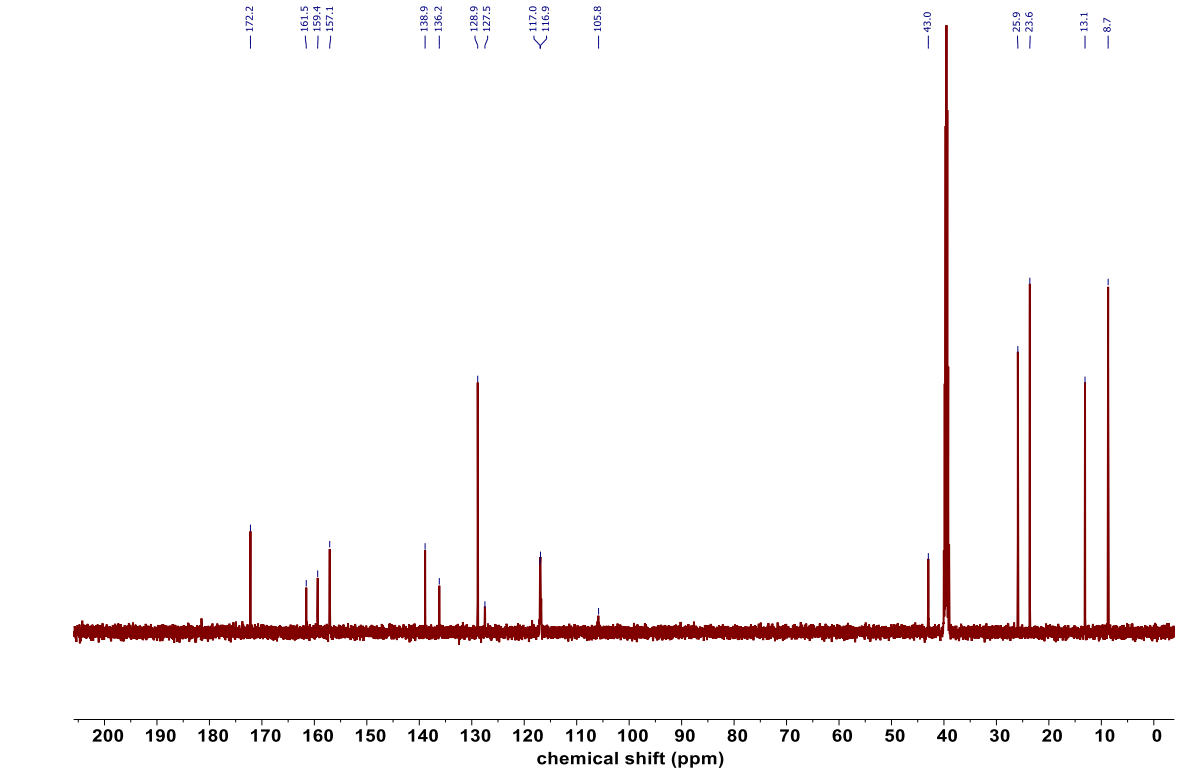

PrOF NMR titrations of small molecules with 5FW BPTF

The PrOF NMR of (**1**) Bromosporine was previously published by our group.[2]

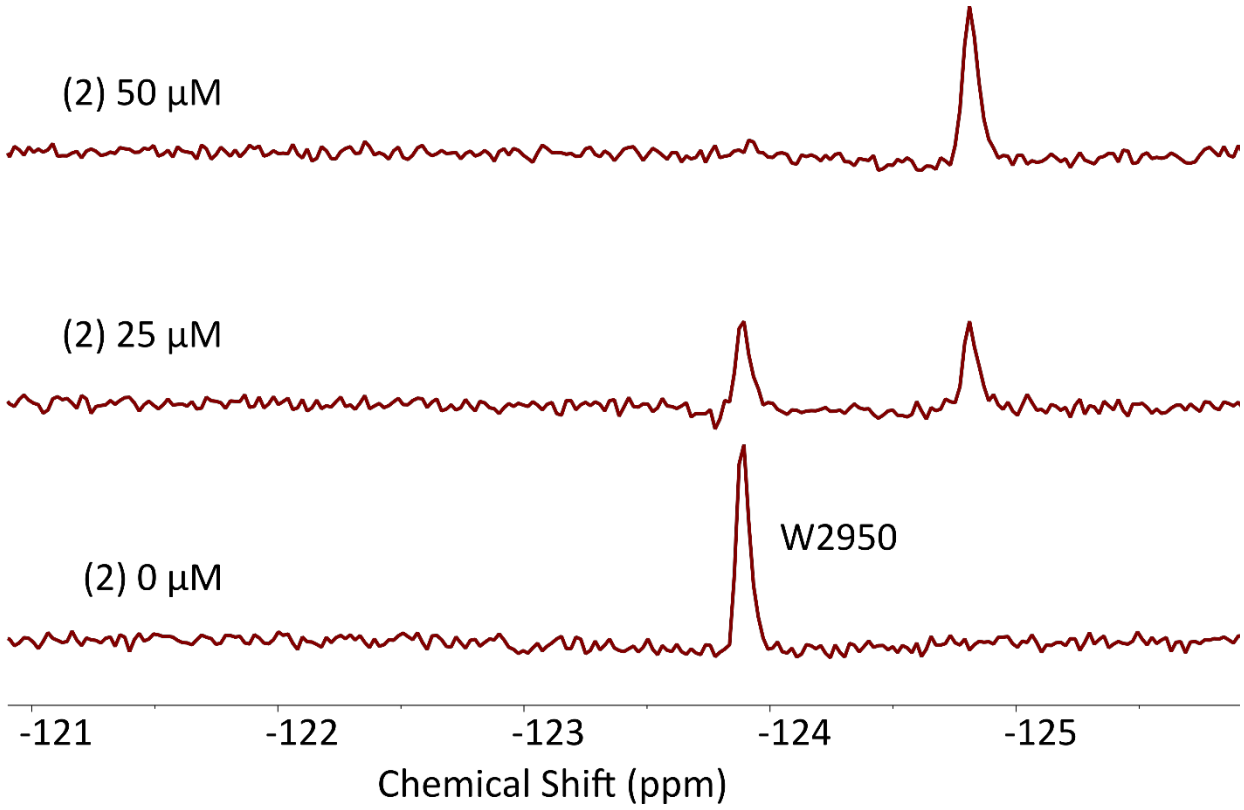

Figure S10: PrOF NMR of (**2**) TP-238: TP-238 displays slow exchange behavior, a bound population resonance grows in at half an equivalent and the fully bound state is observed at saturating equivalents.

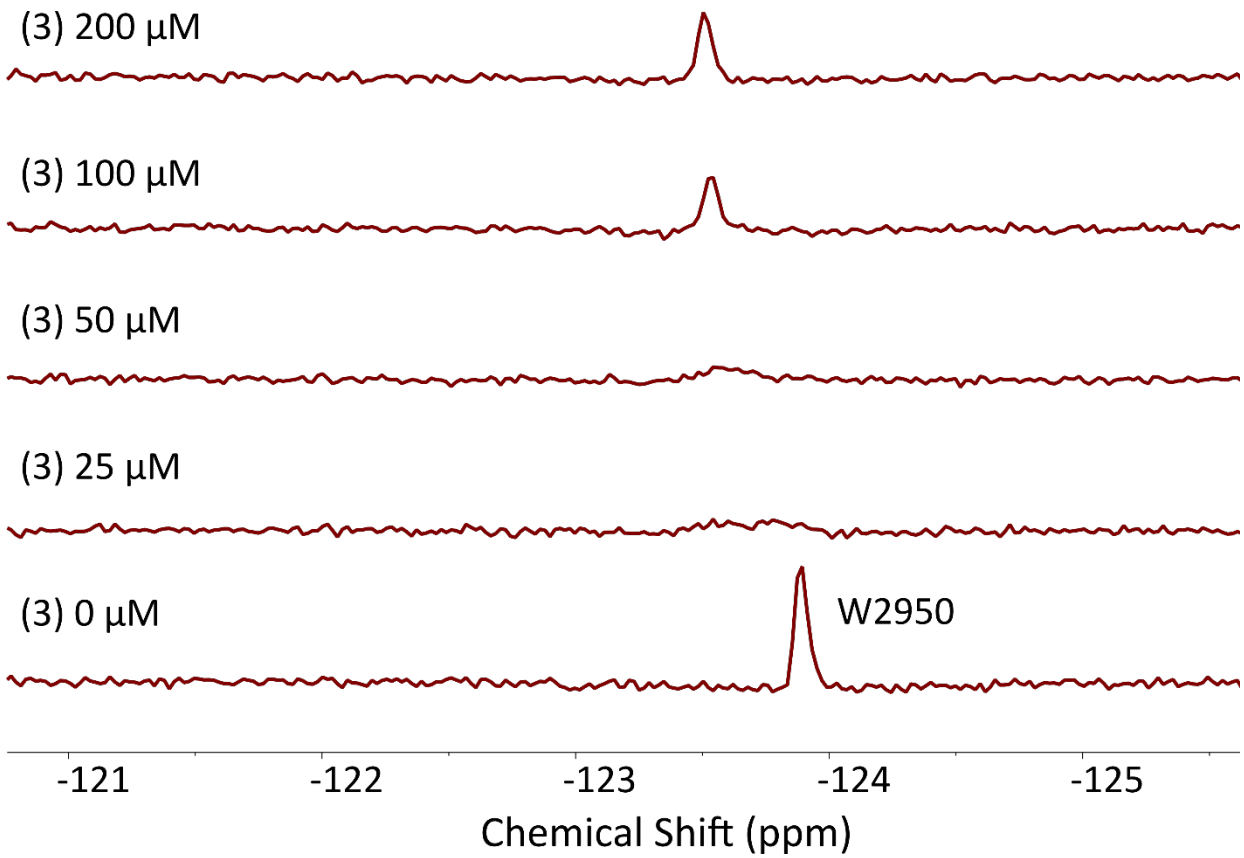

Figure S11: PrOF NMR of (**3**) GSK4027: GSK4027 displays slow-intermediate exchange kinetics, the unbound state broadens to baseline at half an equivalent and the bound population rises from the baseline at superstoichiometric amounts.

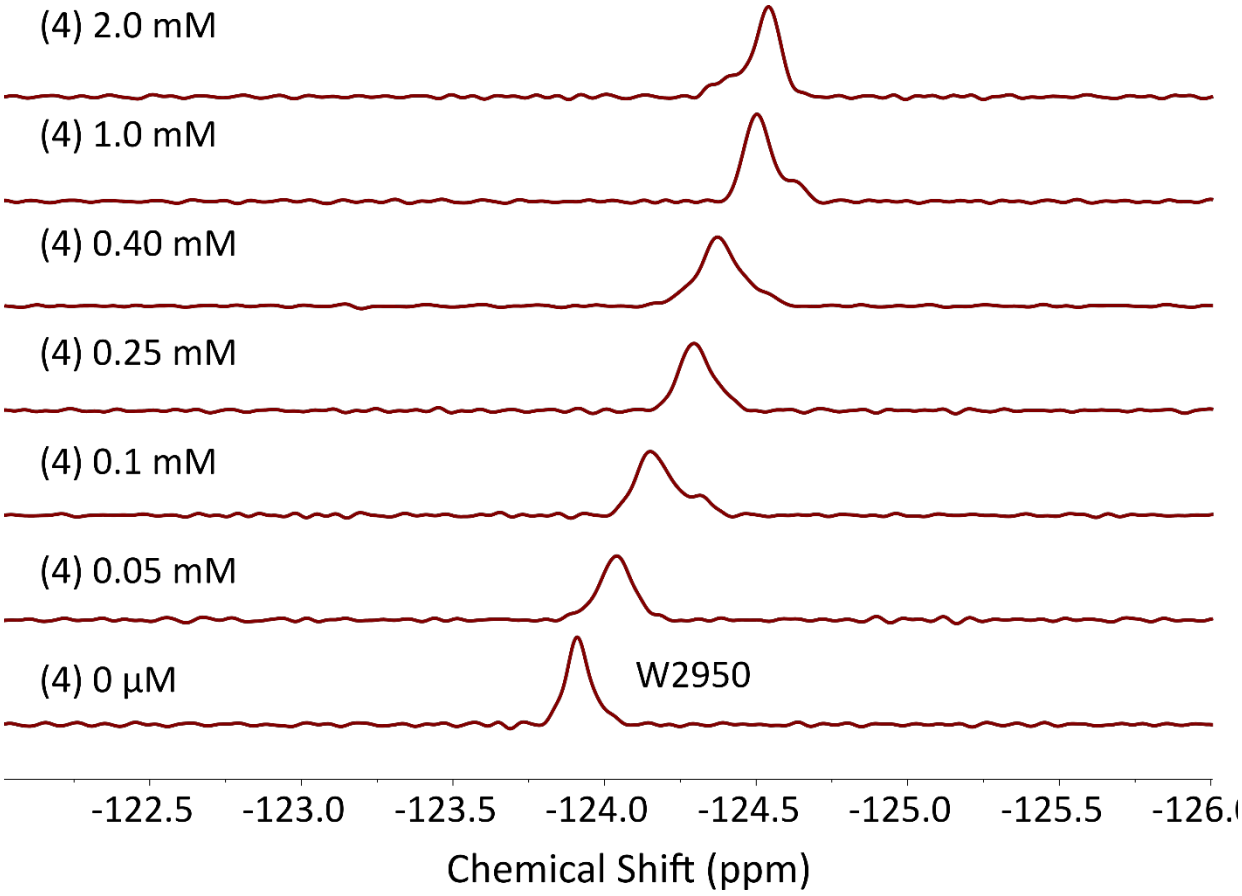

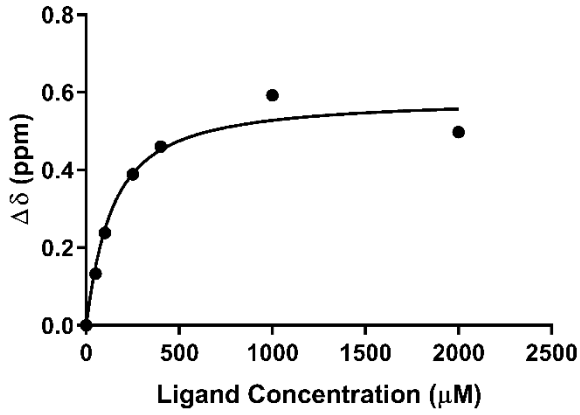

Figure S12: PrOF NMR of (**4**).

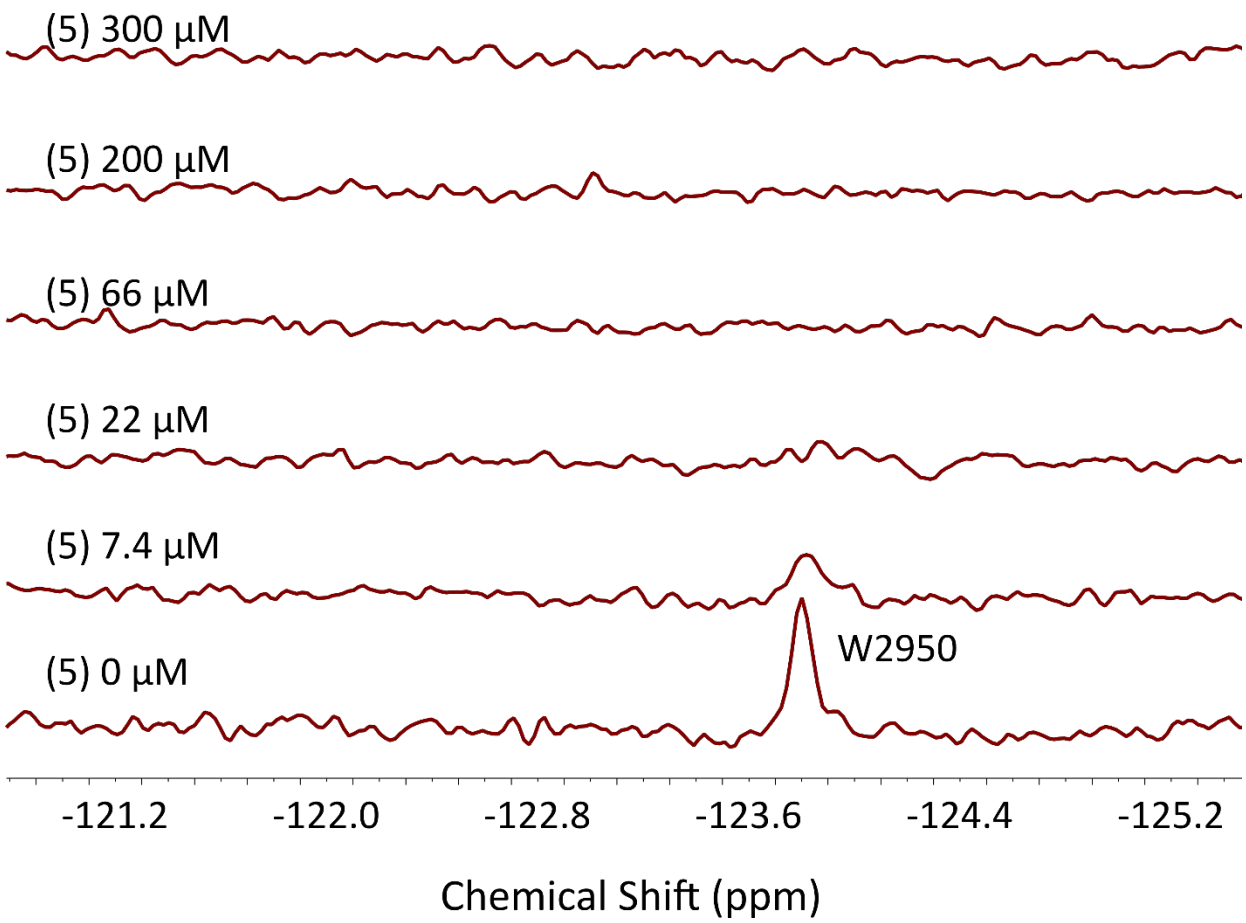

Figure S13: PrOF NMR of (**5**): (**5**) displays intermediate exchange kinetics, a binding isotherm cannot be fit.

a)

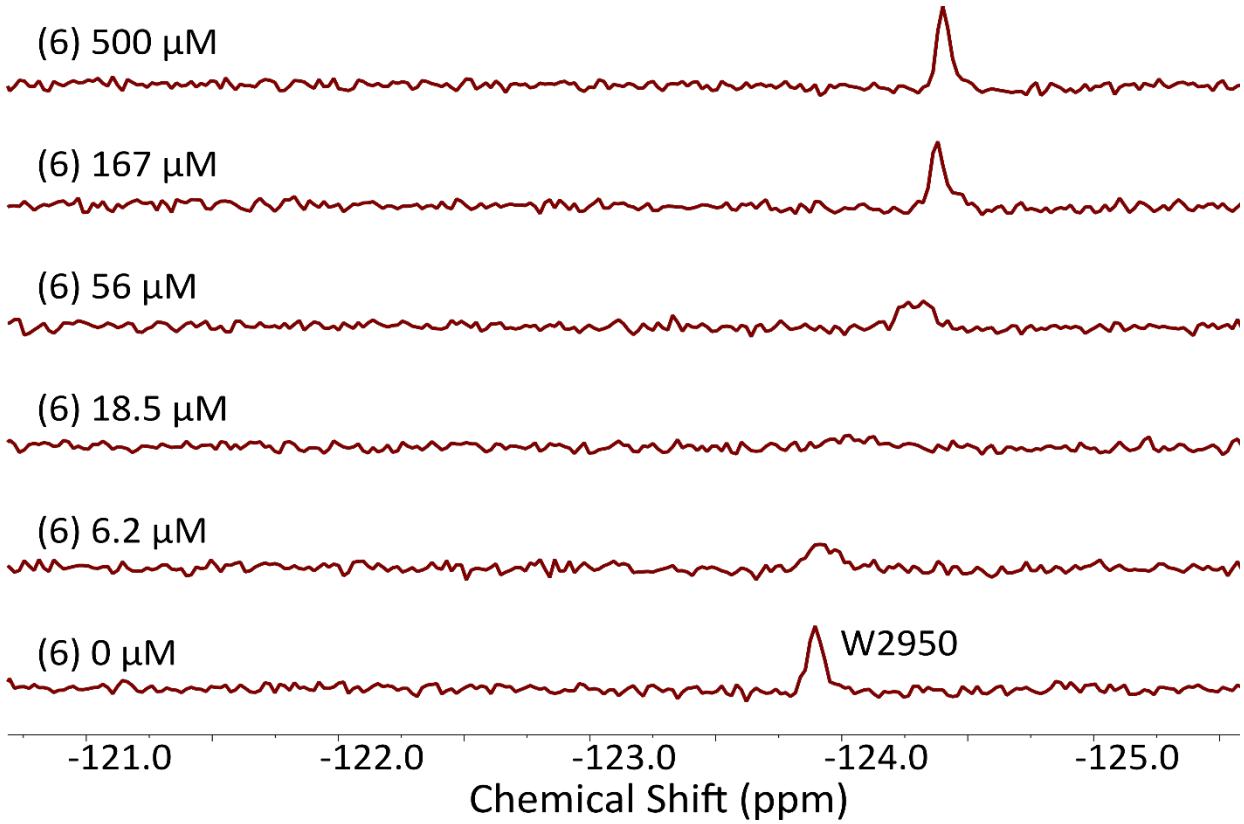

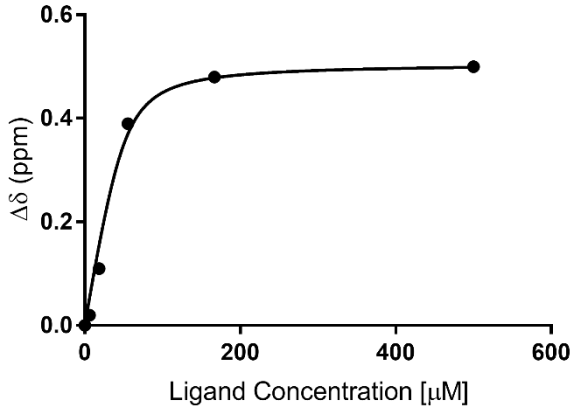

b)

Figure S14: PrOF NMR of (**6**): a) PrOF NMR titration, b) isotherm fit to data in a). This molecule is approaching an affinity where PrOF K_d determinations are less reliable due to the significant broadening of the resonance.

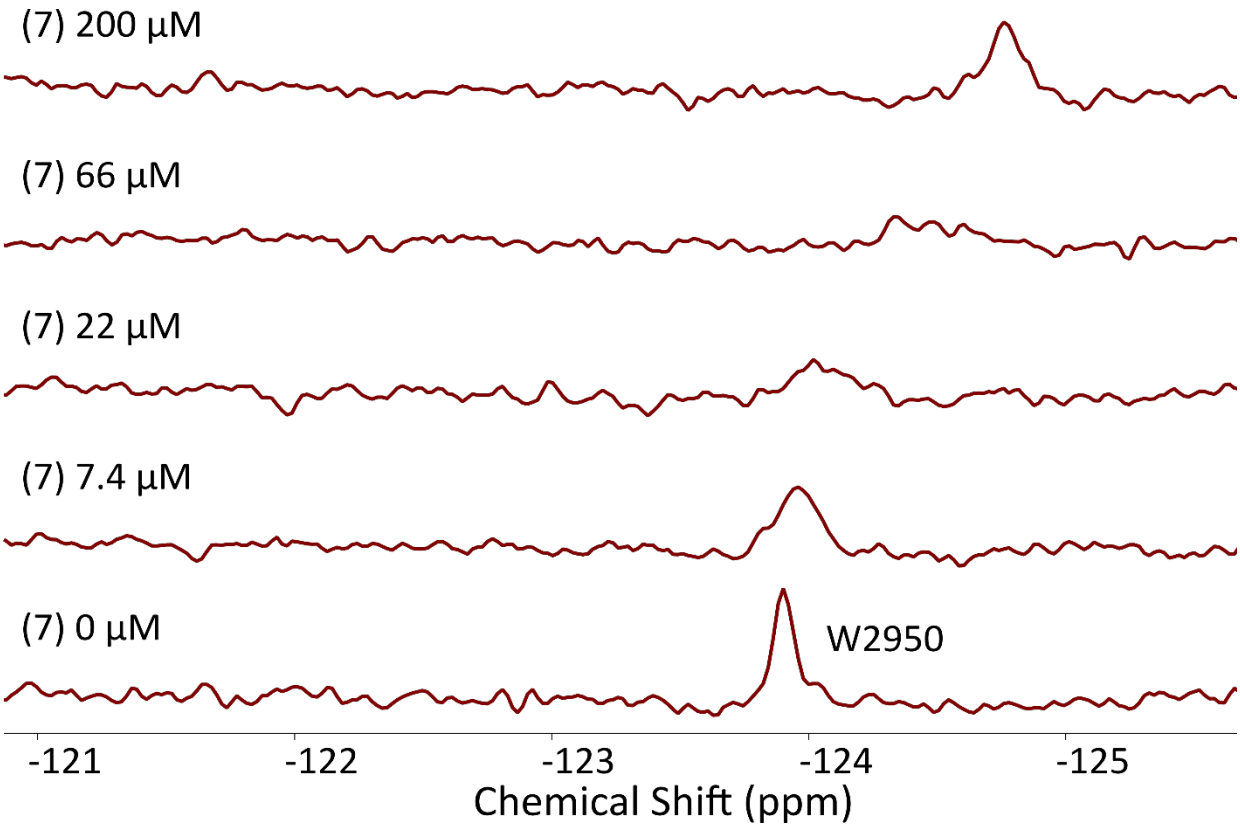

Figure S15: PrOF NMR of (**7**): (**7**) displays intermediate exchange kinetics, a binding isotherm cannot be fit.

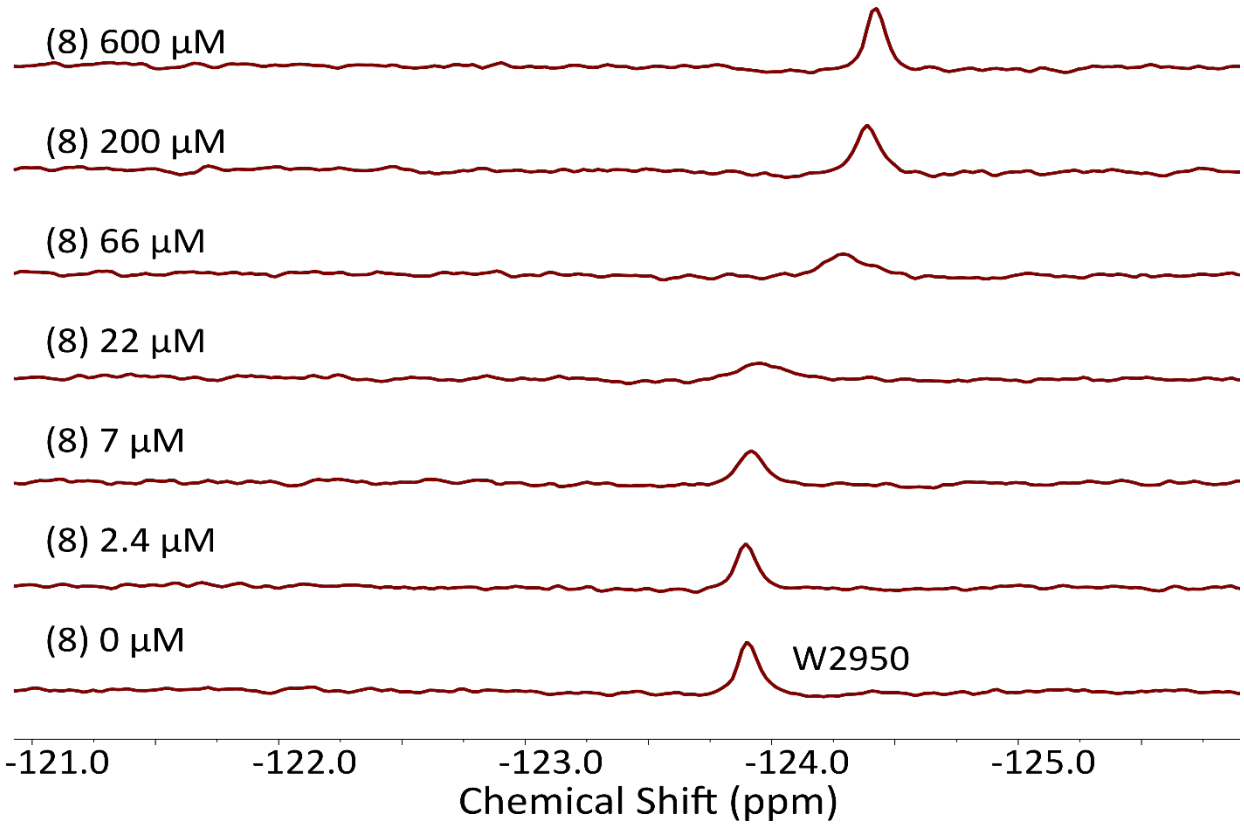

Figure S16: PrOF NMR of (**8**). (**8**) displays intermediate exchange kinetics, a binding isotherm cannot be fit.

a)

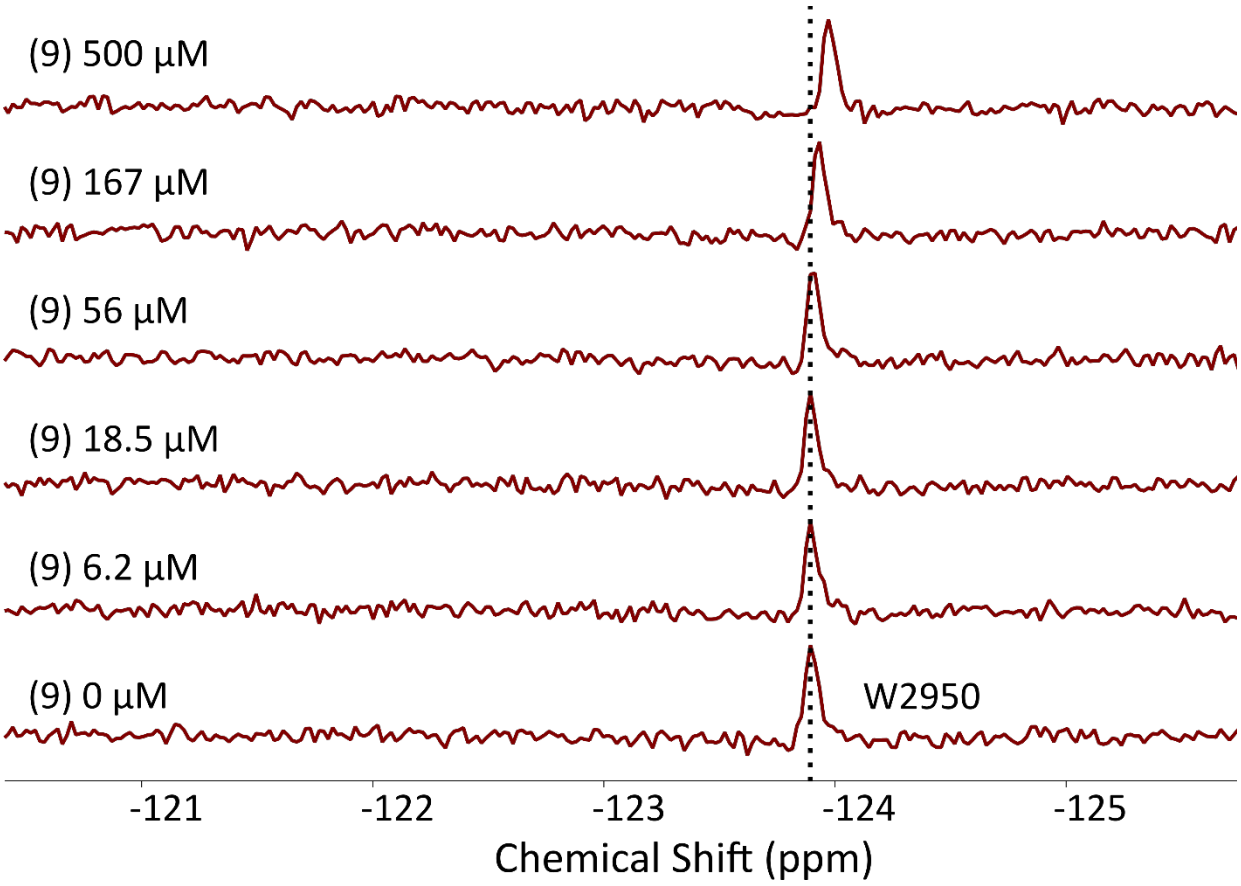

b)

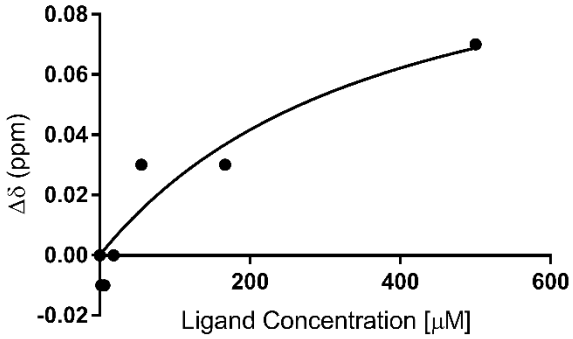

Figure S17: PrOF NMR of (**9**): a) PrOF NMR titration of (**9**) with 5FW-BPTF. b) Binding isotherm generated from data in a). The small dynamic range of the data in a) makes the quantification of K_d by PrOF difficult, evidenced by the poor fit of data in b).

SPR sensorgrams and isotherms for peptides with GST-BPTF

a)

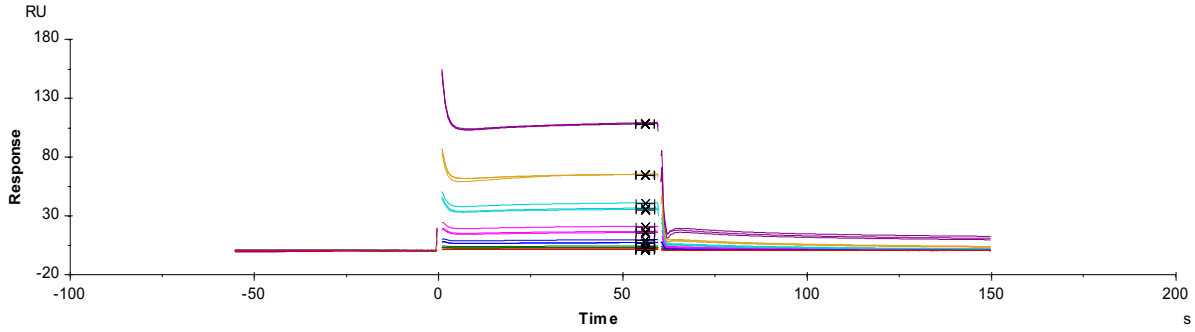

b)

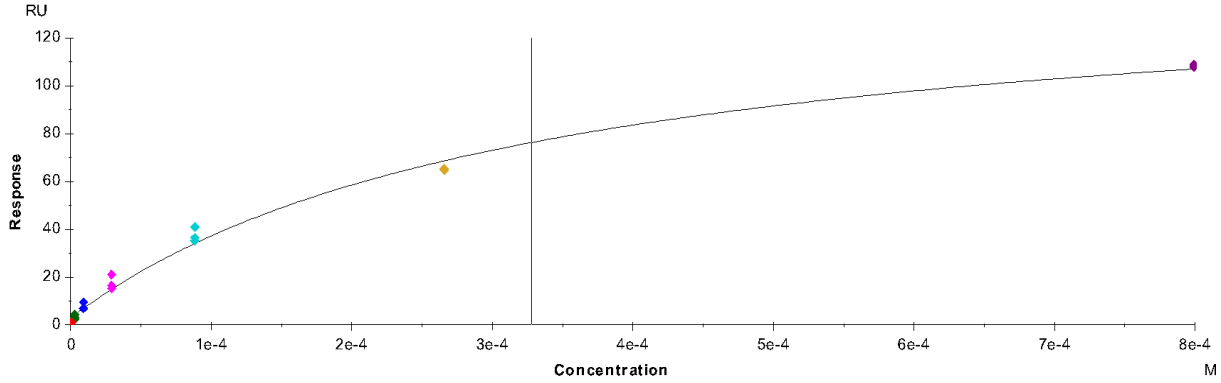

Figure S18: A) SPR titration of H4 $K16_{Ac}$ (Peptide titrated in a 7-step 3-fold serial dilution from 800 µM) ,B) Fit of the binding isotherm

a)

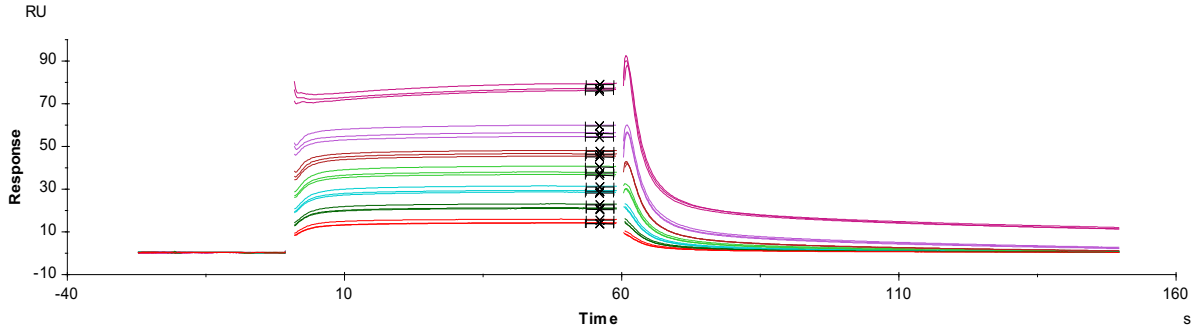

b)

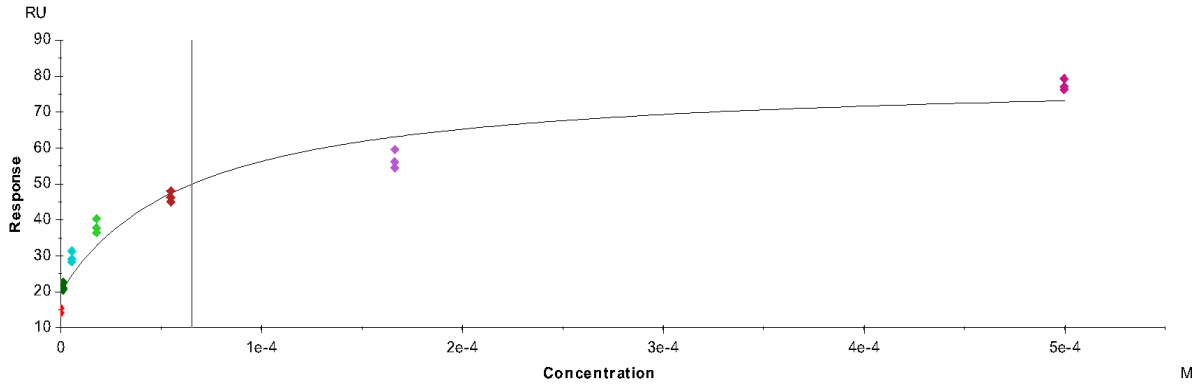

Figure S19: A) SPR titration of H4 $K5_{Ac}$,$K8_{Ac}$,$K12_{Ac}$,$K16_{Ac}$, (Peptide titrated in a 7-step 3-fold serial dilution from 500 µM) B) Fit of the binding isotherm

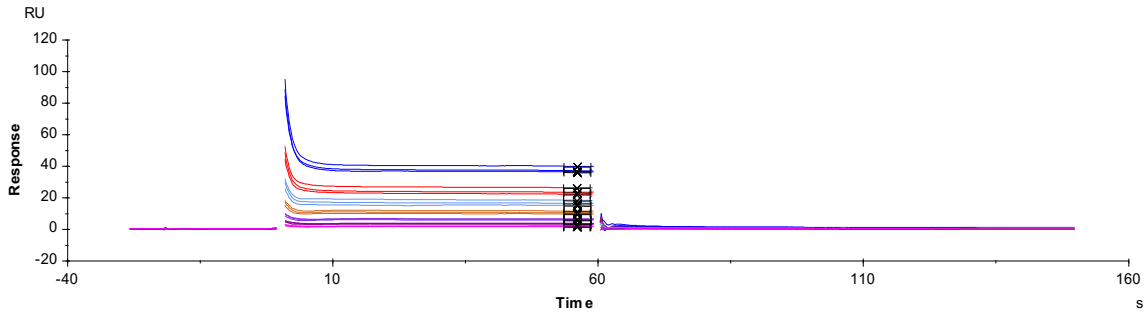

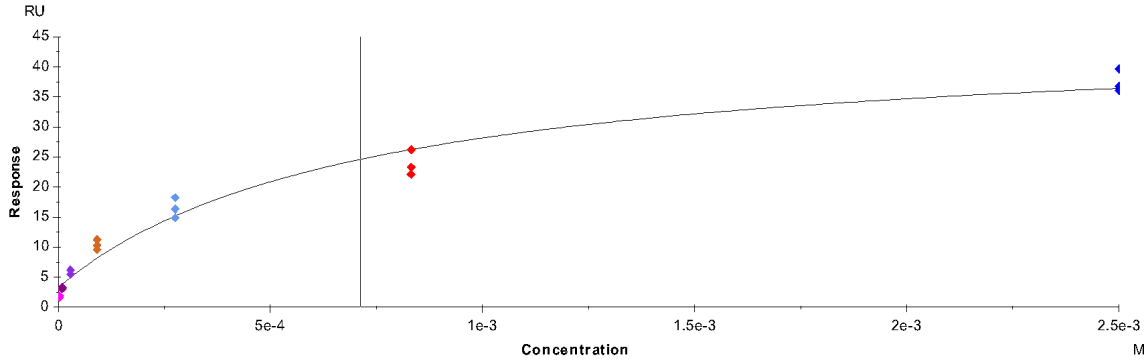

Figure S20: A) SPR titration of H2AZ.I $K4_{Ac}$,$K11_{Ac}$, (Peptide titrated in a 7-step 3-fold serial dilution from 2.5 mM) B) Fit of the binding isotherm

SPR titrations of small molecules with His_9 unlabeled BPTF and His_9 5FW BPTF

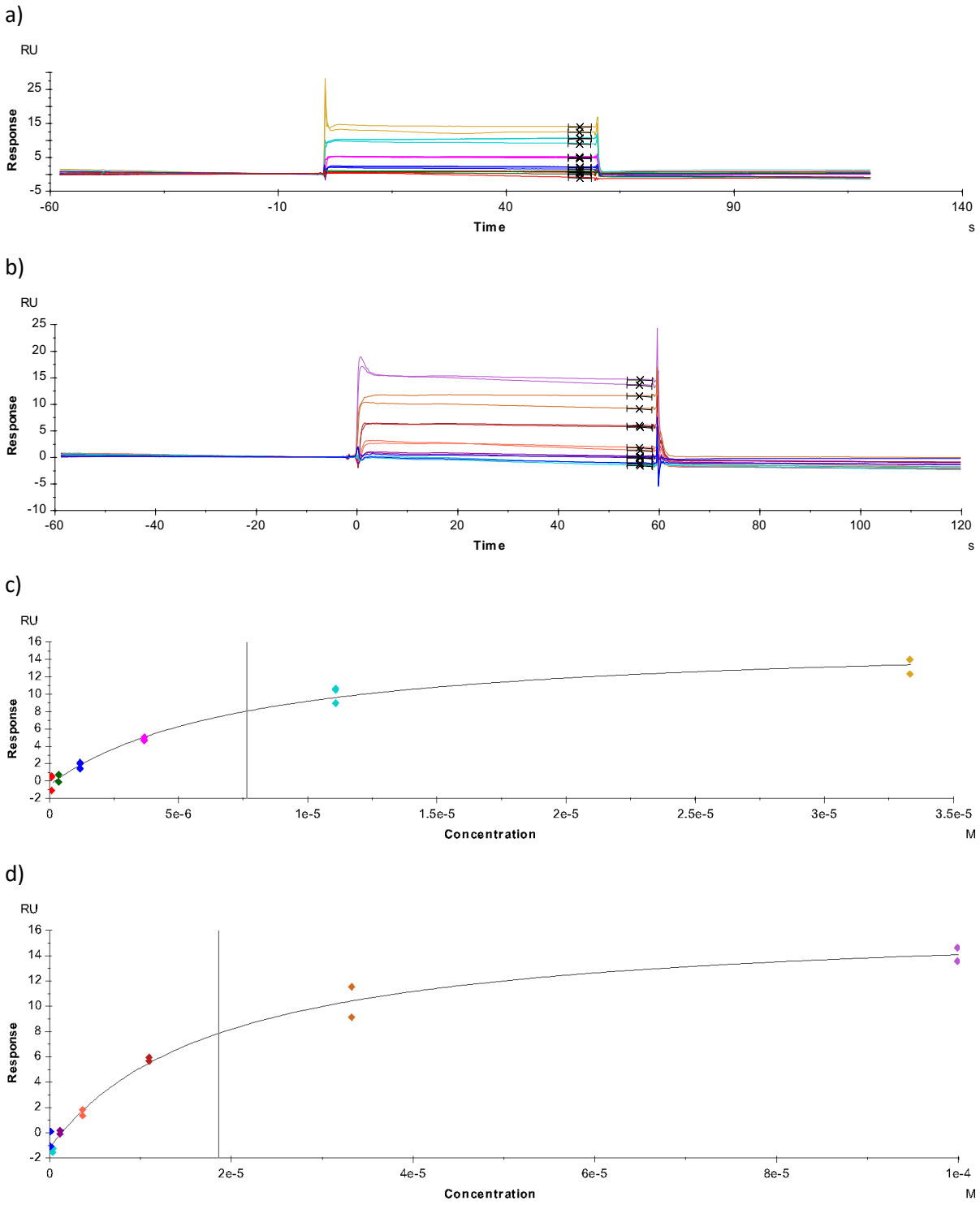

Figure S21: Bromosporine (**1**) titration from 33 µM in a), 11 µM in b) in a three-fold serial dilution: a) SPR sensorgrams from titration with unlabeled-BPTF, b) SPR sensorgrams from titration with 5FW-BPTF, c) binding isotherm from data in a), d) binding isotherm from data in b).

a)

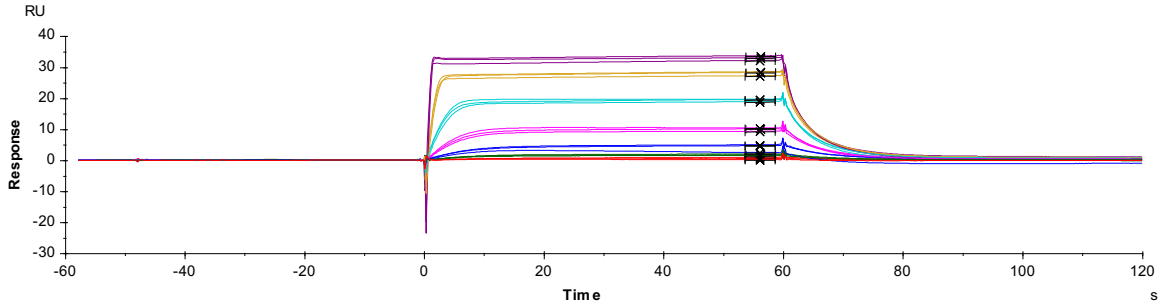

b)

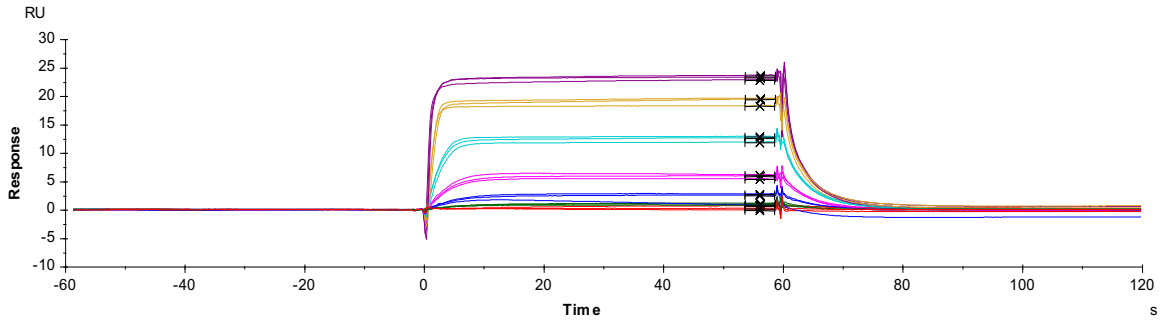

c)

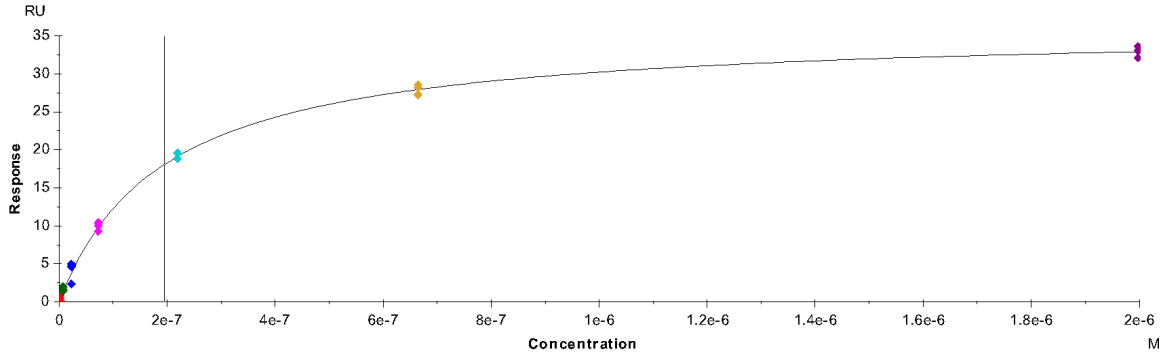

d)

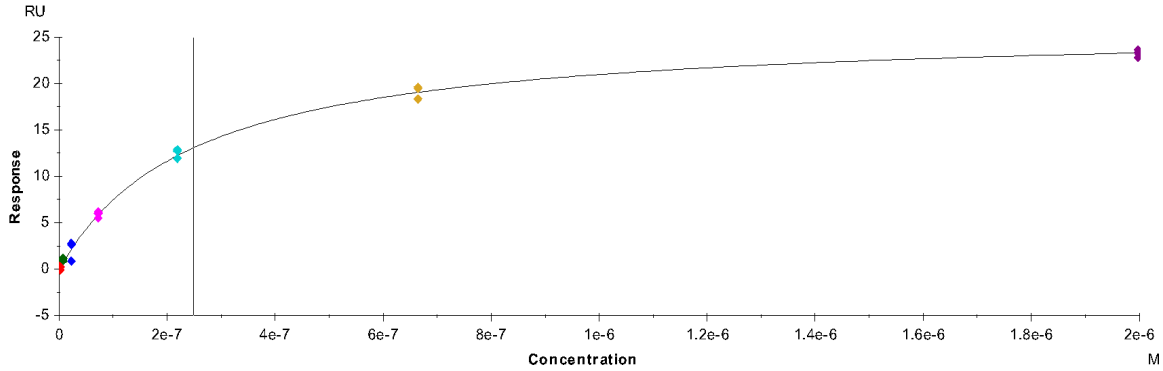

Figure S22: TP-238 (**2**) titration from 2 µM in a 7-step three-fold serial dilution: a) SPR sensorgrams from titration with unlabeled-BPTF, b) SPR sensorgrams from titration with 5FW-BPTF, c) binding isotherm from data in a), d) binding isotherm from data in b).

a)

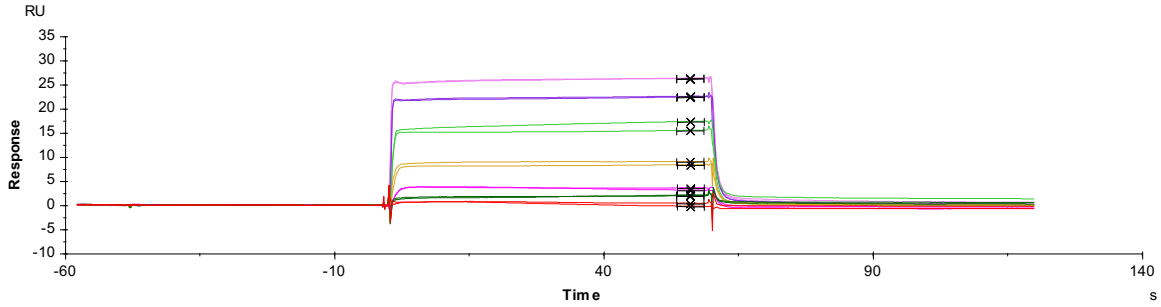
RU
Response
Time
s

b)

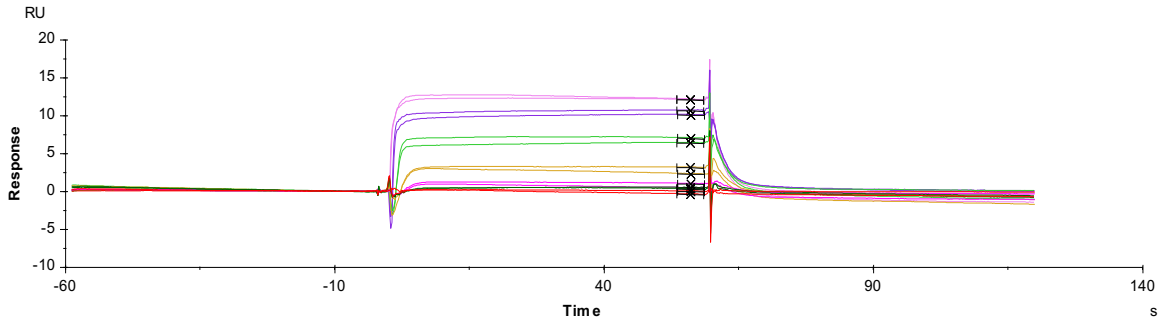
RU
Response
Time
s

c)

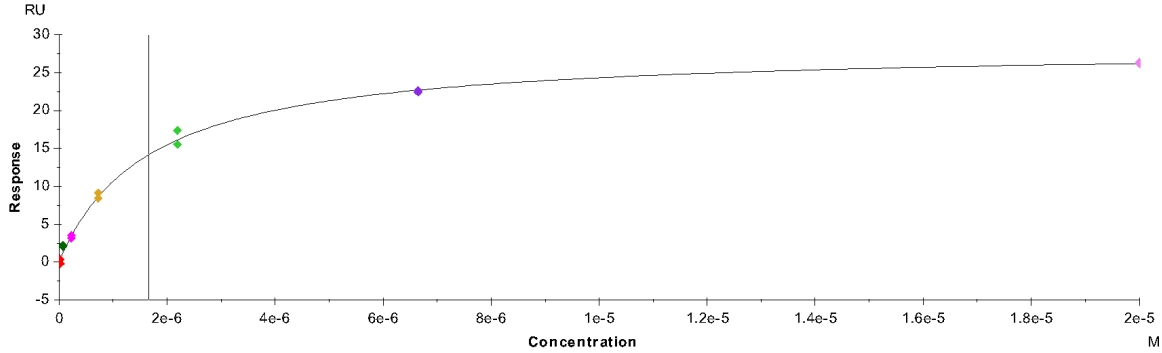
RU
Response
Concentration
M

d)

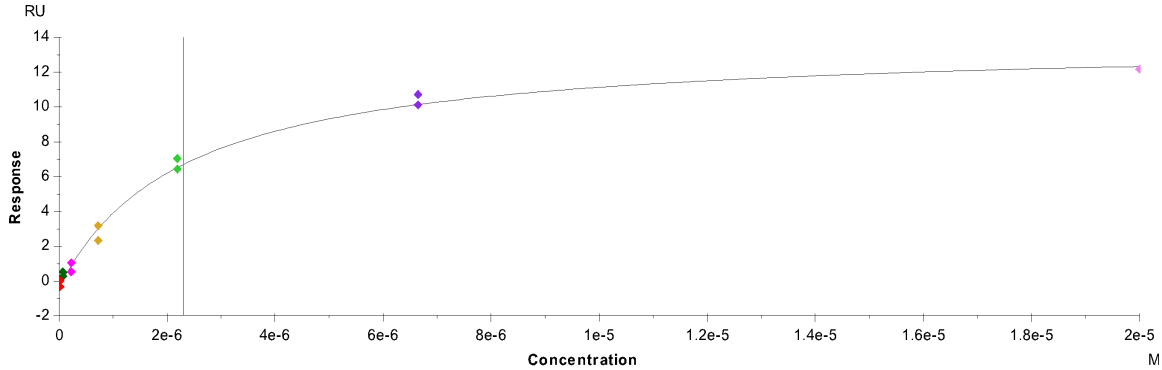
RU
Response
Concentration
M

Figure S23: GSK4027 (**3**) titration from 20 µM in a 7-step three-fold serial dilution: a) SPR sensorgrams from titration with unlabeled-BPTF, b) SPR sensorgrams from titration with 5FW-BPTF, c) binding isotherm from data in a), d) binding isotherm from data in b).

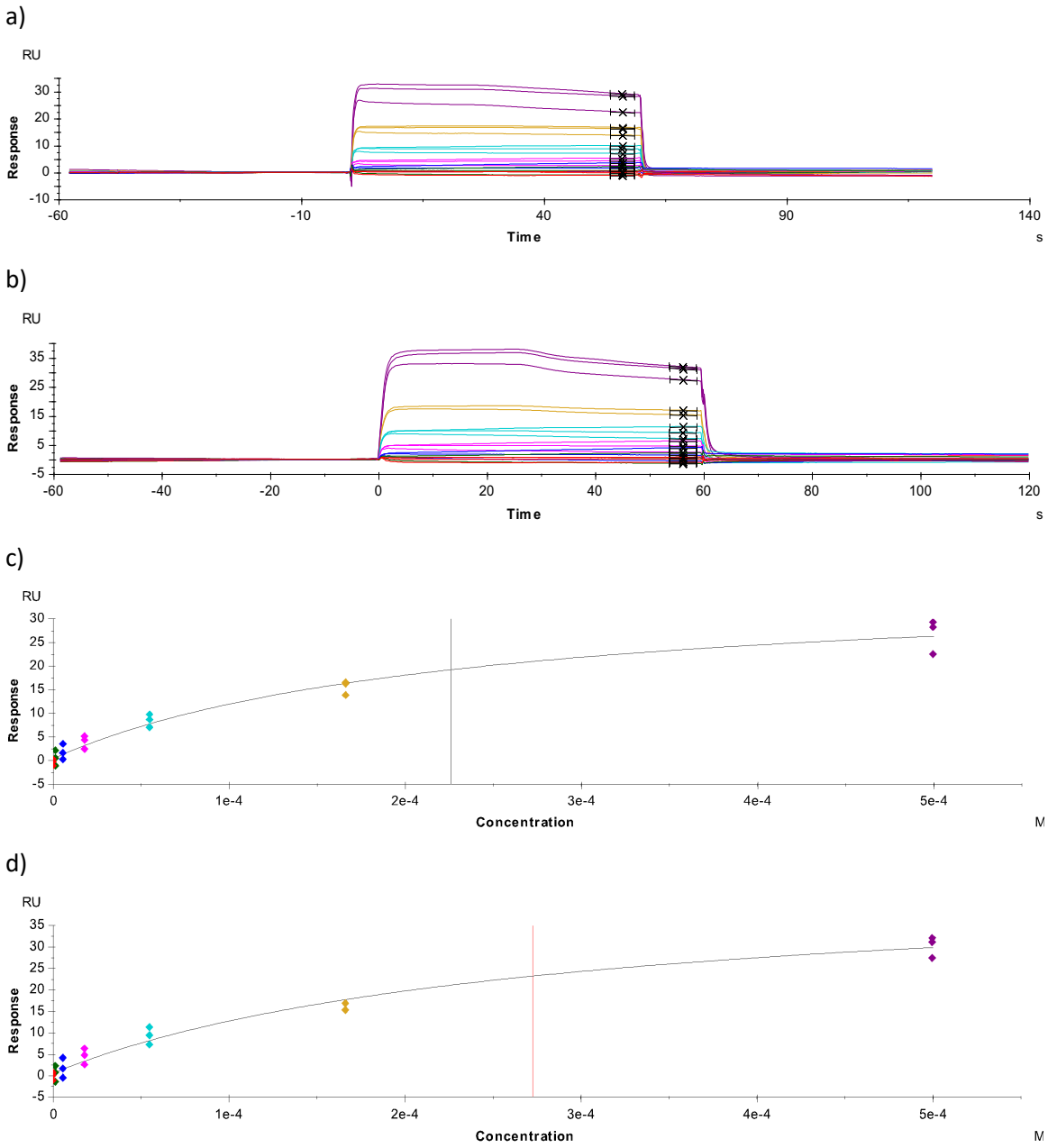

Figure S24: (**4**) titration from 500 µM in a 7-step three-fold serial dilution: a) SPR sensorgrams from titration with unlabeled-BPTF, b) SPR sensorgrams from titration with 5FW-BPTF, c) binding isotherm from data in a), d) binding isotherm from data in b).

(**5**) showed non-specific binding and SPR data could not be collected for this compound

a)

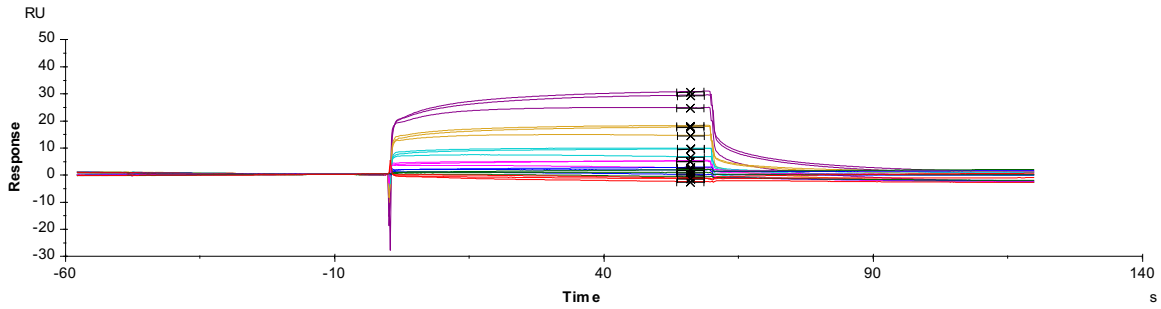

b)

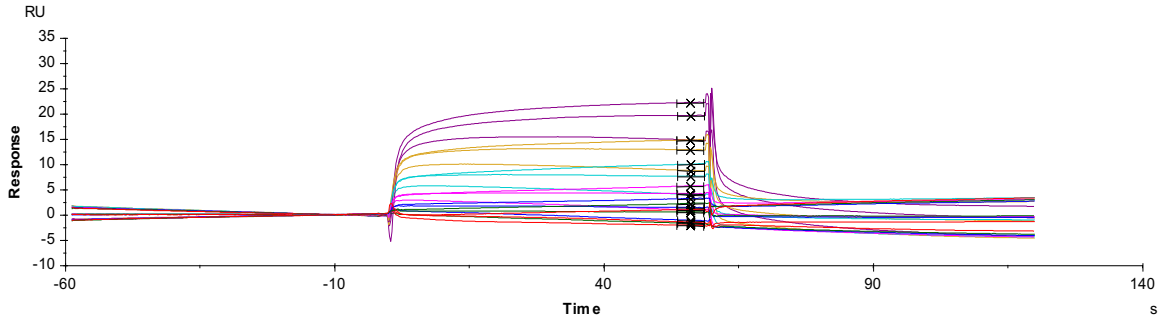

c)

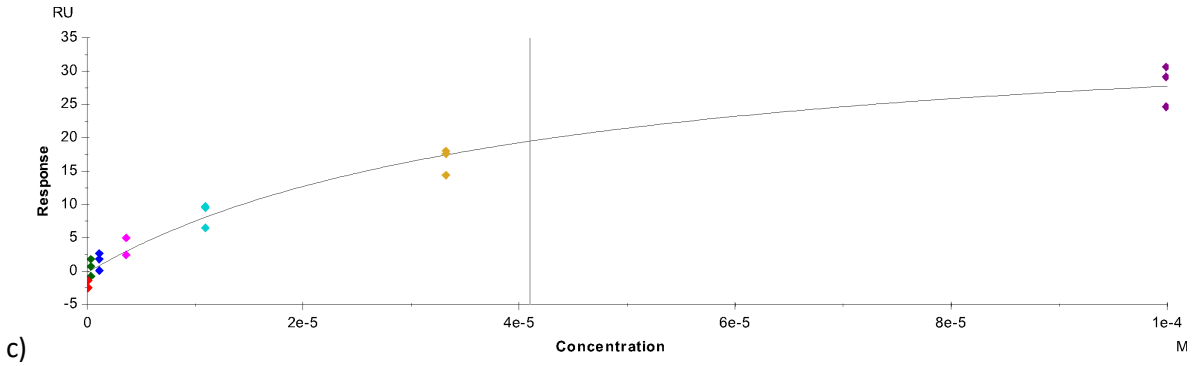

d)

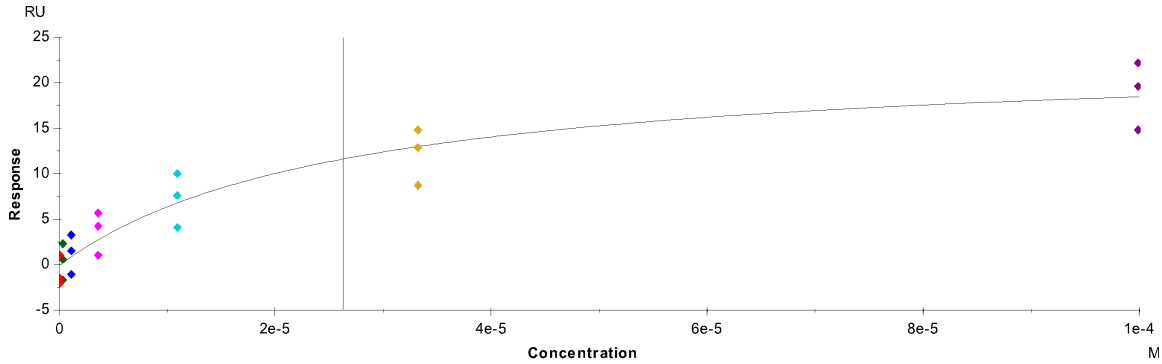

Figure S25: (**6**) titration from 1 mM in a 7-step three-fold serial dilution: a) SPR sensorgrams from titration with unlabeled-BPTF, b) SPR sensorgrams from titration with 5FW-BPTF, c) binding isotherm from data in a), d) binding isotherm from data in b).

a)

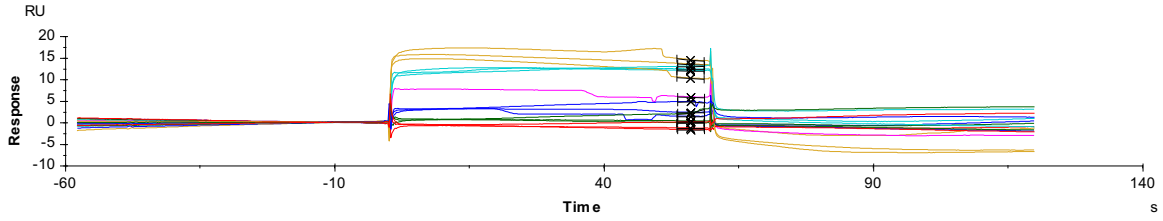

b)

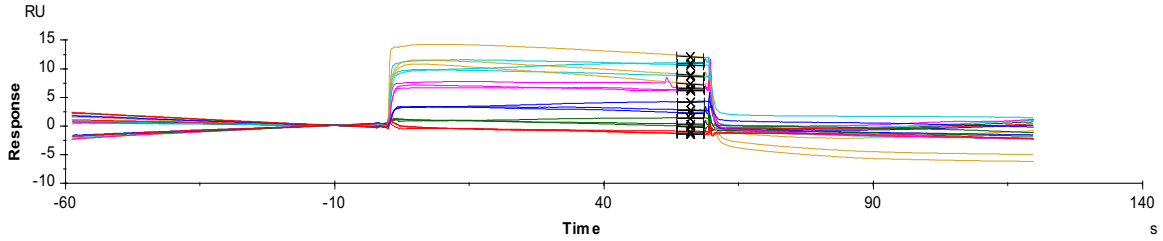

c)

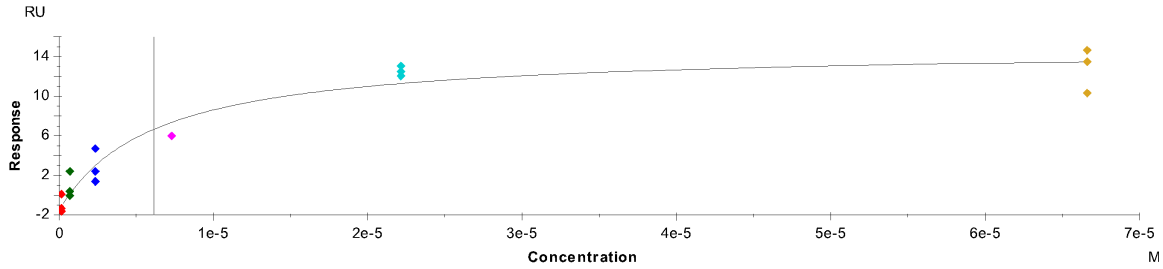

d)

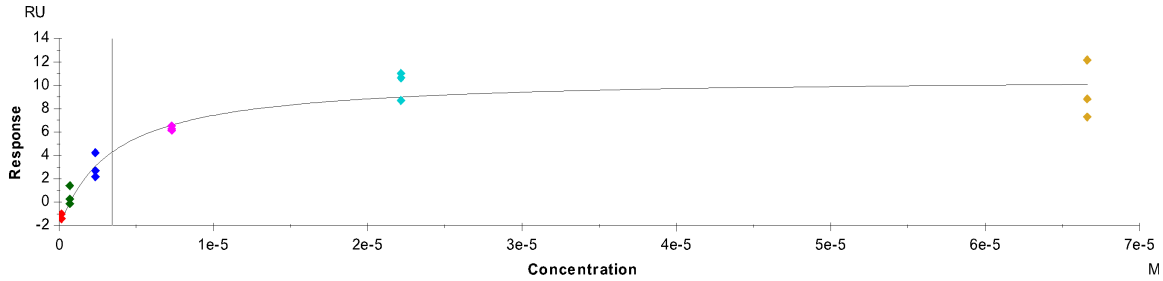

Figure S26: (**7**) titration from 667 µM in a 7-step three-fold serial dilution: a) SPR sensorgrams from titration with unlabeled-BPTF, b) SPR sensorgrams from titration with 5FW-BPTF (displays binding to reference channel at high concentrations), c) binding isotherm from data in a), d) binding isotherm from data in b).

a)

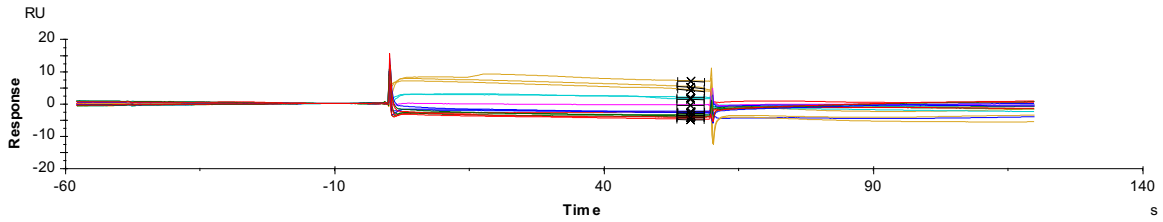

b)

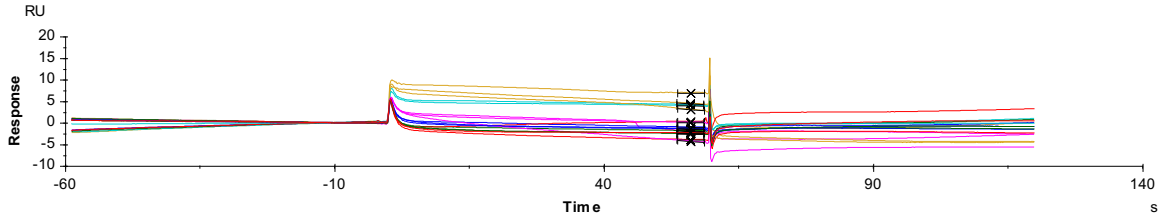

c)

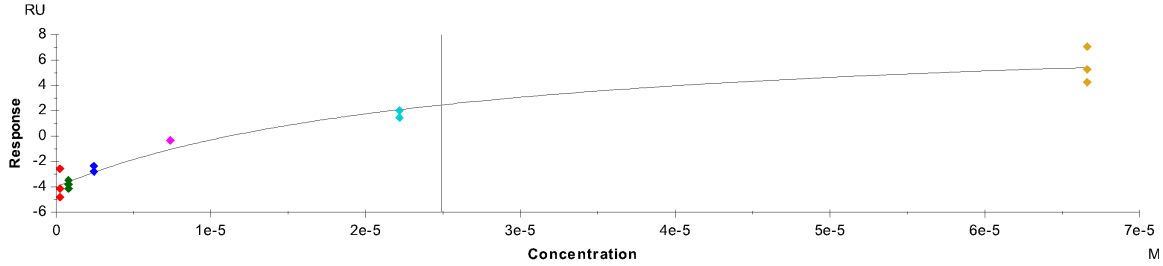

d)

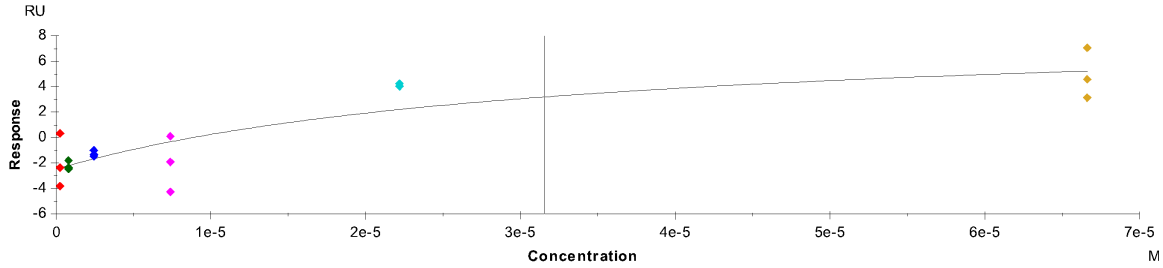

Figure S27: (**8**) titration from 667 µM in a 7-step three-fold serial dilution: a) SPR sensorgrams from titration with unlabeled-BPTF(displays binding to reference channel at high concentrations), b) SPR sensorgrams from titration with 5FW-BPTF (displays binding to reference channel at high concentrations), c) binding isotherm from data in a), d) binding isotherm from data in b).

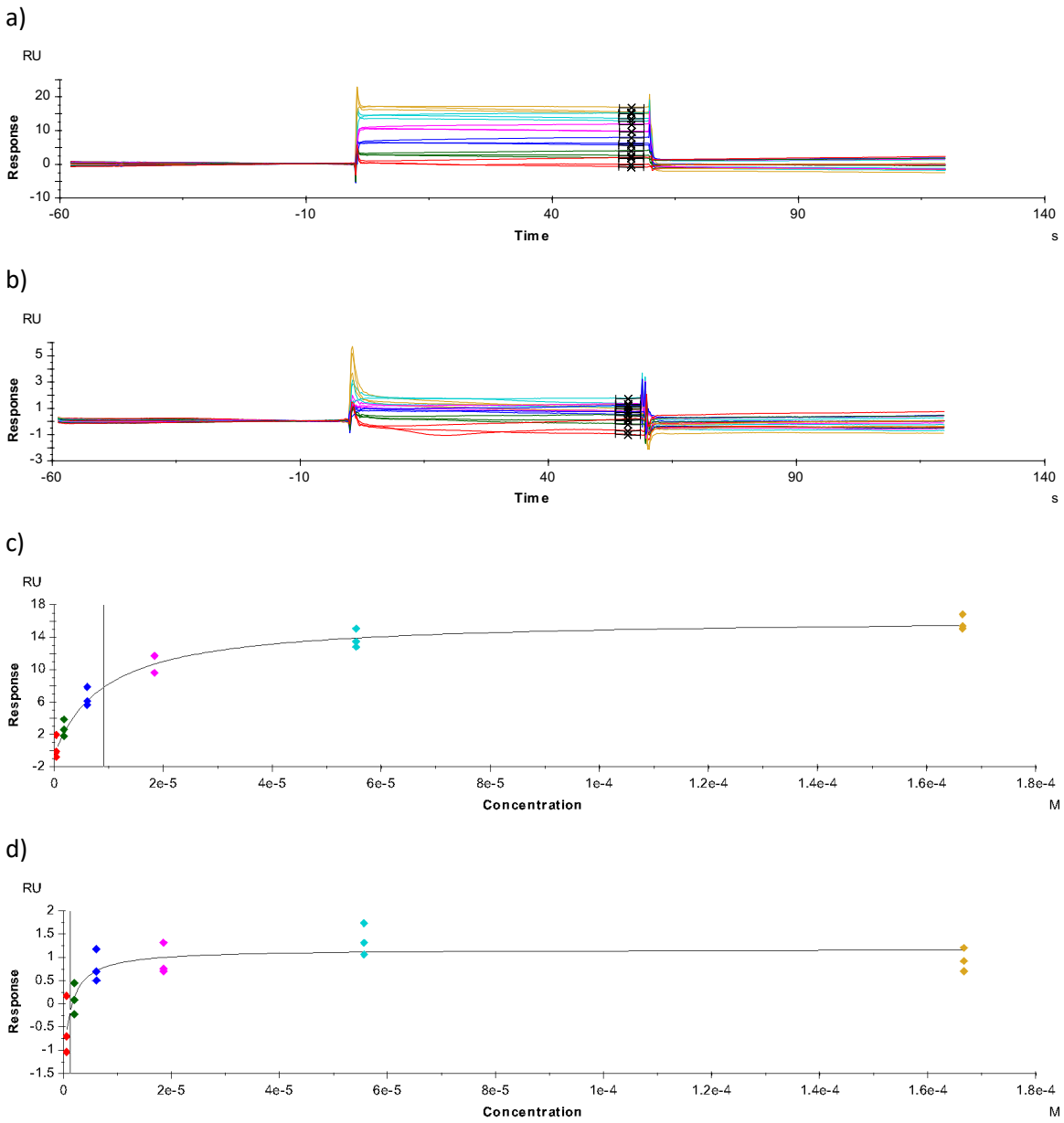

Figure S28: (**9**) titration from 167 µM in a 6-step three-fold serial dilution: a) SPR sensorgrams from titration with unlabeled-BPTF, b) SPR sensorgrams from titration with 5FW-BPTF, c) binding isotherm from data in a), d) binding isotherm from data in b). Due to binding of (**9**) to the reference channel at high ligand concentrations, dissociation constants could not be accurately determined.

SPR titrations of small molecules 1-3 with GST-BPTF

Table S4: SPR K_d values for molecules **1**-**3** with GST-tagged BPTF (mean and standard deviation of technical triplicates)

Compound	GST-BPTF SPR K_d
Bromosporine (**1**)	6 ± 0.7 µM
TP-238 (**2**)	260 ± 30 nM
GSK4027 (**3**)	1.5 ± 0.5 µM

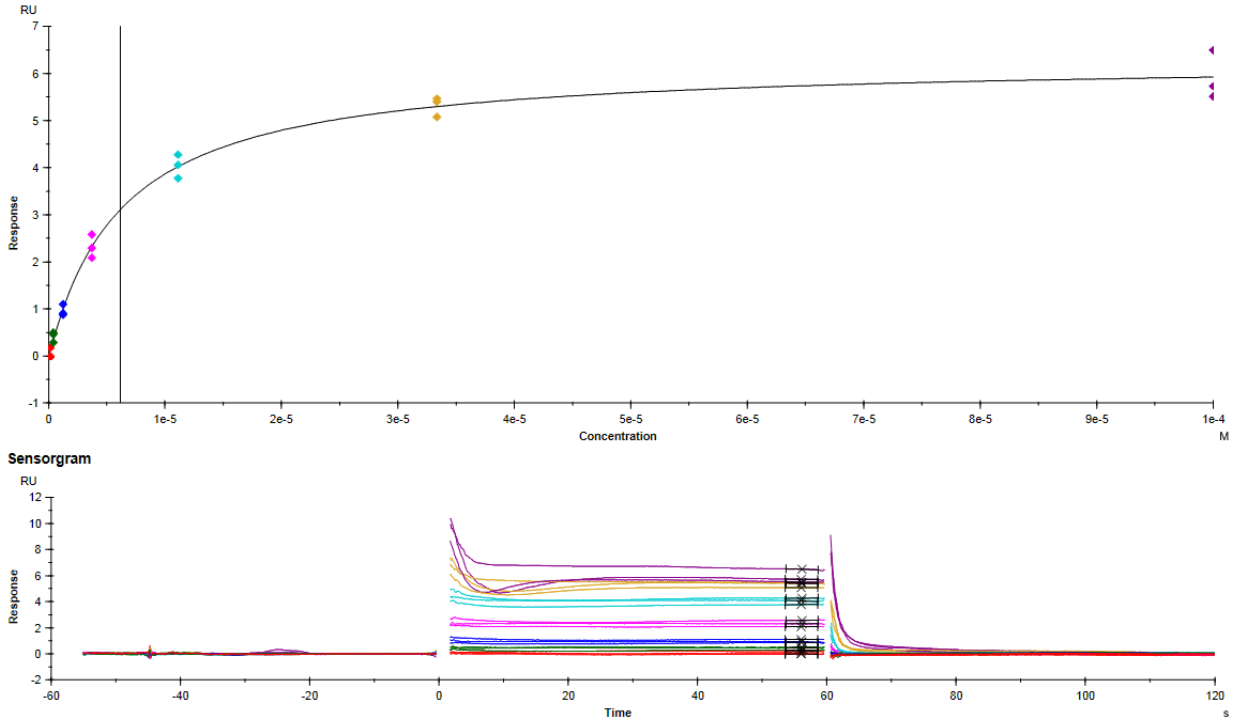

Figure S29: Bromosporine (**1**) titration from 100 µM in a 7-step three-fold serial dilution: (top) SPR binding isotherm and (bottom) sensorgram of titration with GST-BPTF

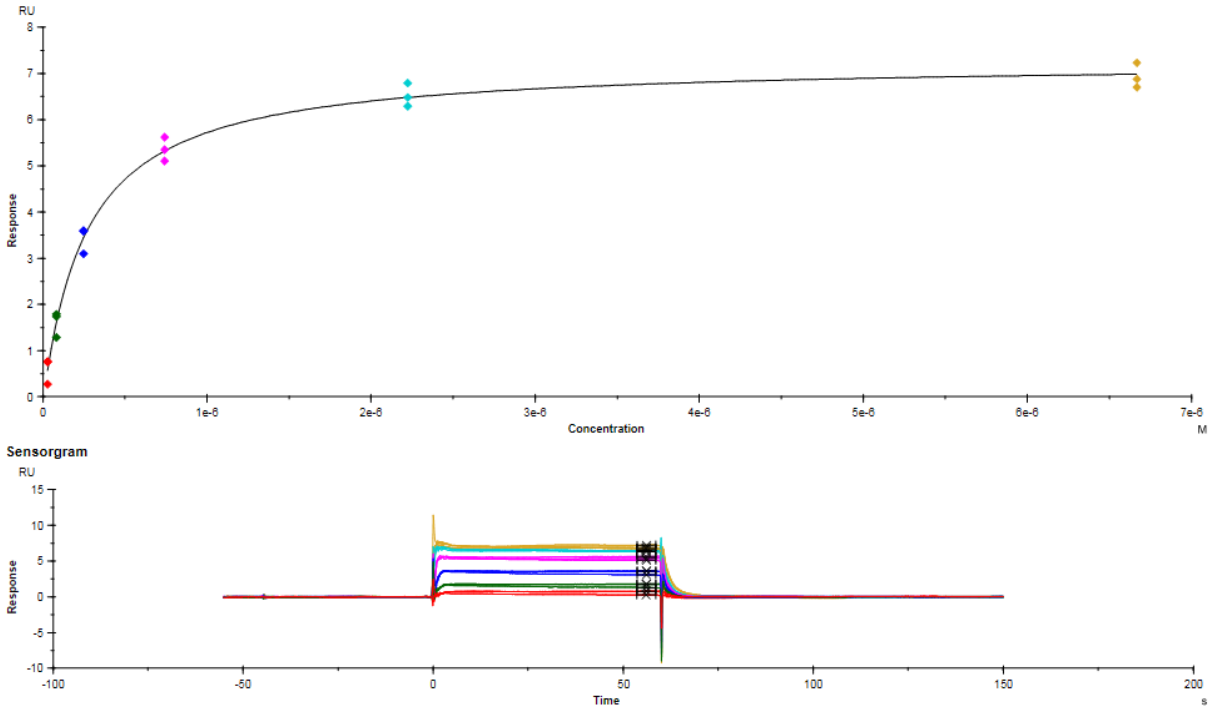

Figure S30: TP-238 (**2**) titration from 6.7 µM in a 6-step three-fold serial dilution: (top) SPR binding isotherm and (bottom) sensorgram of titration with GST-BPTF

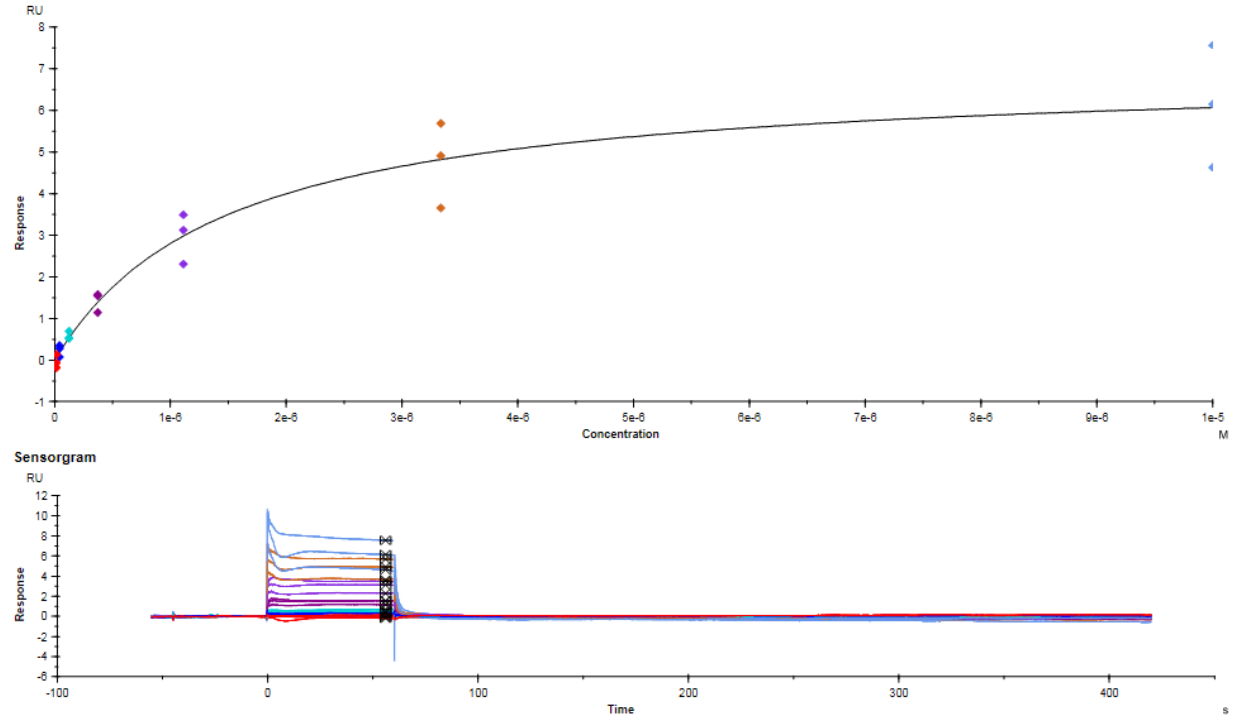

Figure S31: GSK4027 (**3**) titration from 10 µM in a 7-step three-fold serial dilution: (top) SPR binding isotherm and (bottom) sensorgram of titration with GST-BPTF

AlphaScreen titrations of small molecules with His_9 BPTF

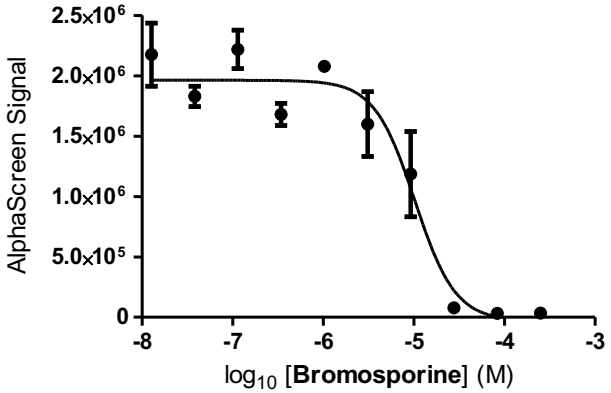

Figure S32: AlphaScreen titration of **1** (Bromosporine) with BPTF

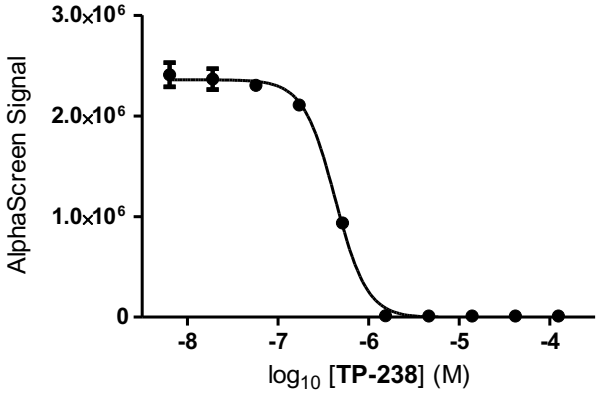

Figure S33: AlphaScreen titration of **2** (TP-238) with BPTF

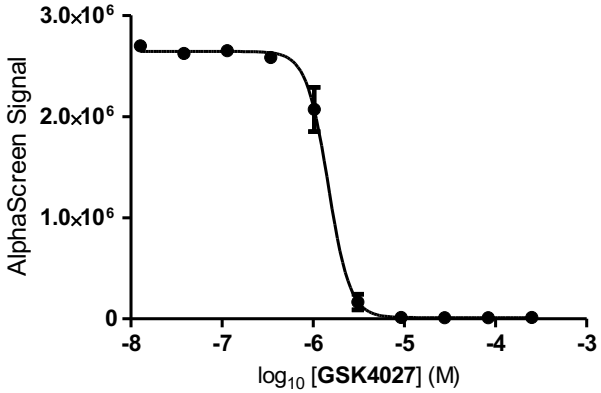

Figure S34: AlphaScreen titration of **3** (GSK4027) with BPTF

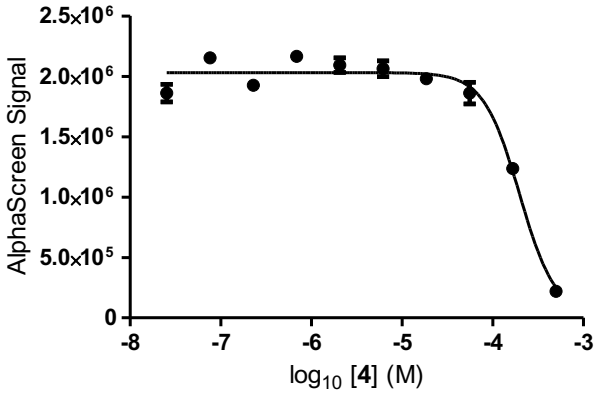

Figure S35: AlphaScreen titration of **4** with BPTF. Baseline constraint applied using compound **8**.

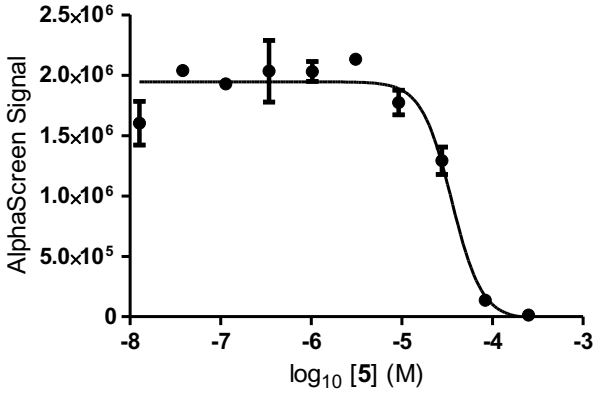

Figure S36: AlphaScreen titration of **5** with BPTF

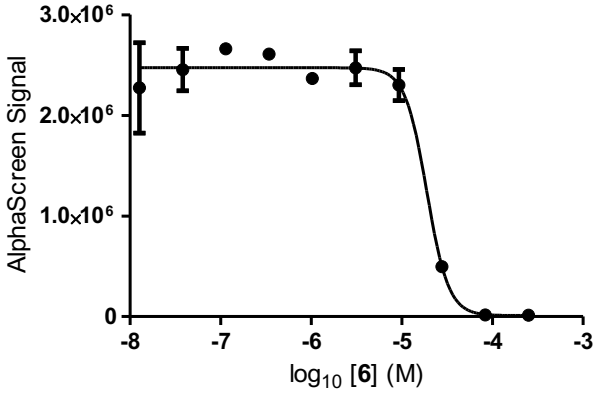

Figure S37: AlphaScreen titration of **6** with BPTF

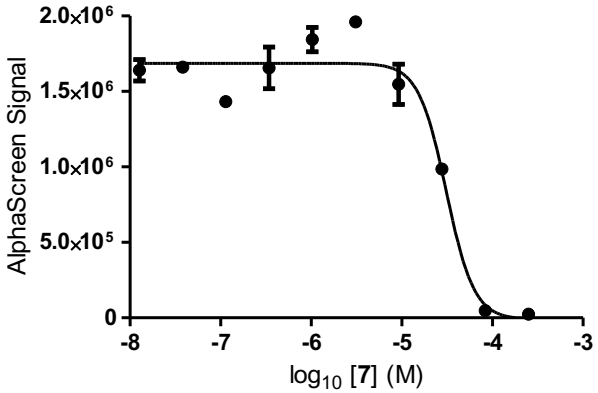

Figure S38: AlphaScreen titration of **7** with BPTF

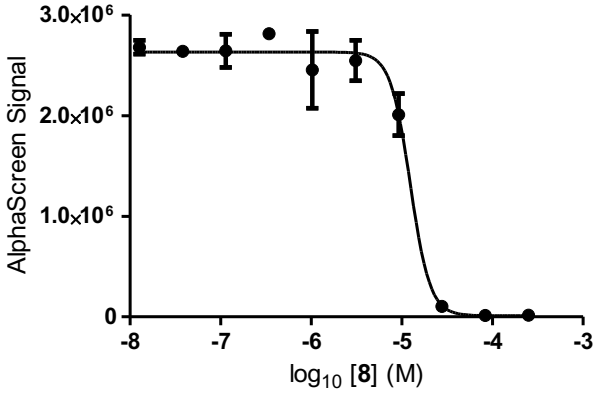

Figure S39: AlphaScreen titration of **8** with BPTF

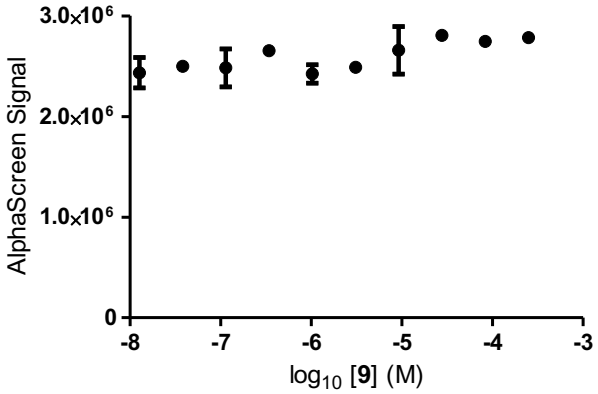

Figure S40: AlphaScreen titration of **9** with BPTF. Non-binding up to 250 µM of the compound.

X-ray Crystallography data

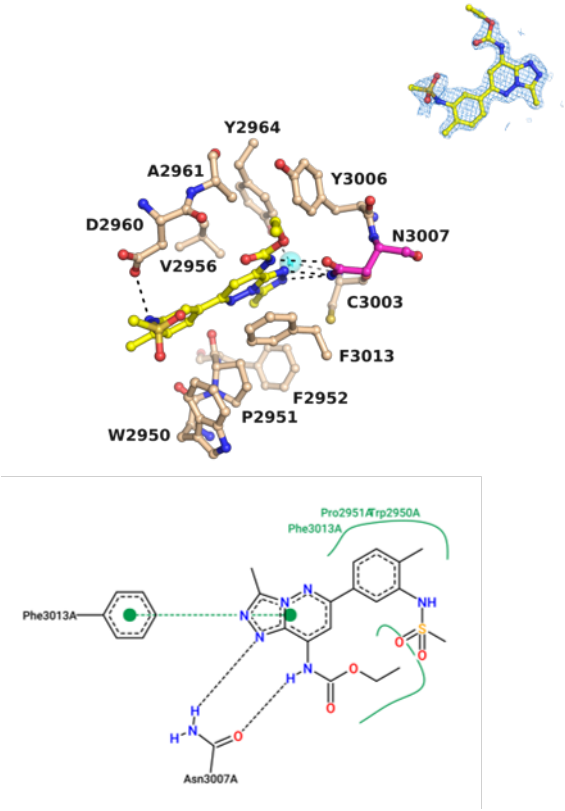

Figure S41:. BPTF Bromodomain cocrystal structure with bromosporine (**1**). BPTF residues and bromosporine are depicted in beige and yellow, respectively. Potential H-bonding interactions include conserved N3007 (magenta) in the acetylated lysine binding pocket (black dotted lines, 2.2 < d < 3.5 Å). Potential hydrophobic VDW interactions are indicated with green wiggled lines and Pi-Pi interactions with F3013 green dotted lines with distance cut-off 3.3 < d < 4.0 Å. A cyan sphere shows a bound water molecule. The blue mesh around the inhibitor shows the corresponding 2Fo-Fc electron density map contoured at 1σ. Water mediated H-bonds were excluded from the interaction schematics for clarity.

Table S5: Data collection and refinement statistics

Inhibitor	**GSK4027 (3)**		**5**	**4**	**TP-238 (2)**	**Bromosporine (1)**
Data collection						
Space group	P 1		P 1	C 1 2 1	P 43 21 2	C 1 2 1
Unit cell dimensions	a	27.06	27.22	111.45	42.62	111.66
	b	35.52	37.96	27.27	42.62	27.15
	c	41.15	57.07	38.03	126.71	38.41
	α	114	97	90	90	90
	β	96	104	97	90	97.927
	γ	91	91	90	90	90
Resolution range (Å)	31.77 - 1.6		33.02 - 1.71	33.09 - 1.13	31.7 - 1.54	38.04 - 1.67

	(1.657 - 1.6)		(1.771 - 1.71)	(1.17 - 1.13)	(1.595 - 1.54)	(1.73 - 1.67)
Unique reflections	17234 (1700)		23628 (2311)	42137 (4168)	18156 (1775)	13515 (1327)
Rmeas (%)	5 (30.8)		22.2 (46.0)	6.3 (56)	7.7 (96.1)	5.2 (51.6)
Completeness (%)	94.1 (93.25)		99.34 (99.01)	98.13 (97.38)	99.77 (99.89)	99.65 (99.48)
I/σI	12.84 (3.37)		11.82 (3.02)	14.13 (3.07)	18.45 (3.13)	19.83 (3.07)
Structure refinement						
Rwork (%)	17.81 (19.94)		20.69 (30.97)	19.17 (25.59)	19.35 (24.04)	17.47 (23.25)
Rfree[a] (%)	21.94 (22.70)		24.42 (39.35)	20.02 (29.17)	21.84 (24.77)	20.80 (27.18)
Wilson B (Å^2)	16.8		17.0	13.6	21.4	18.0
Average B (Å²)	all	22.0	25.9	20.7	28.5	25.3
	protein	21.1	25.8	19.7	28.1	24.3
	ligand	22.9	29.4	30.0	22.5	44.2
	solvent	29.4	26.8	28.9	36.2	29.55
rmsd[b] bond lengths (Å)	0.006		0.006	0.005	0.005	0.006
rmsd angles (deg)	0.81		0.80	0.80	0.75	0.78
Ramachandran	favored (%)	99.17	99.10	99.14	100.00	100
	allowed (%)	0.83	0.90	0.86	0.00	0.00
	outliers (%)	0	0	0	0	0

Values in parenthesis are for the highest resolution bins.
[a] Rfree is Rcryst calculated for randomly chosen unique reflections.
[b] rmsd = root-mean-square deviation from ideal values, which were excluded from the refinement.

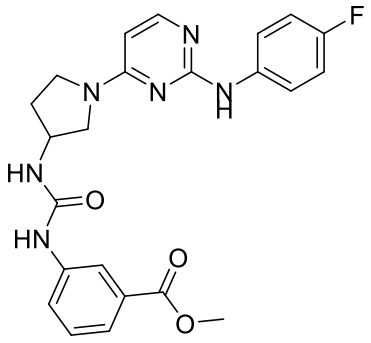

AU1

Ligand Efficiency = 0.22

K_d = 2.8 μM

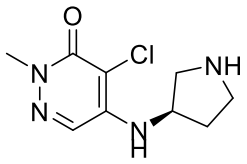

8

Ligand Efficiency = 0.50

K_d = 3 μM

Figure S42: Comparison of ligand efficiency of previously studied molecule (AU1) and fragment molecule studied here, (**8**).

[1] Humphreys, P. G.; Bamborough, P.; Chung, C. W.; Craggs, P. D.; Gordon, L.; Grandi, P.; Hayhow, T. G.; Hussain, J.; Jones, K. L.; Lindon, M.; Michon, A. M.; Renaux, J. F.; Suckling, C. J.; Tough, D. F.; Prinjha, R. K. Discovery of a Potent, Cell Penetrant, and Selective P300/CBP-Associated Factor (PCAF)/General Control Nonderepressible 5 (GCN5) Bromodomain Chemical Probe. *J. Med. Chem.* **2017**, *60* (2), 695–709.

[2] Perell, G. T.; Mishra, N. K.; Sudhamalla, B.; Ycas, P. D.; Islam, K.; Pomerantz, W. C. K., Specific Acetylation Patterns of H2A.Z Form Transient Interactions with the BPTF Bromodomain. *Biochemistry* **2017,** *56* (35), 4607-4615.